COPY

# REPORT DOCUMENTATION PAGE

AFRL-SR-BL-TR-01-

0227



| 1. REPORT DATE (DD-MM-YYYY) | 2. REPORT TYPE | 3. DATES COVERED (From - To) |
|---|---|---|
| 20-03-2001 | Final Technical Report | 15-12-1997 - 31-12-2000 |

**4. TITLE AND SUBTITLE**

A Rational Approach to the Design and Synthesis of Tough Glassy Polymers

**5a. CONTRACT NUMBER**

**5b. GRANT NUMBER**
F49620-98-1-0158

**5c. PROGRAM ELEMENT NUMBER**

**6. AUTHOR(S)**

Yee, Albert F.

**5d. PROJECT NUMBER**
2303/CV

**5e. TASK NUMBER**

**5f. WORK UNIT NUMBER**

**7. PERFORMING ORGANIZATION NAME(S) AND ADDRESS(ES)**
The University of Michigan
3003 S. State St.
Room 1058
Ann Arbor, MI 48109-1274

**8. PERFORMING ORGANIZATION REPORT NUMBER**

**9. SPONSORING/MONITORING AGENCY NAME(S) AND ADDRESS(ES)**
AFOSR/NL
Dr. Charles Y-C. Lee, Program Officer
110 Duncan Ave Room B115
Bolling AFB, DC 20332-8050

**10. SPONSOR/MONITOR'S ACRONYM(S)**
AFOSR/NL

**11. SPONSORING/MONITORING AGENCY REPORT NUMBER**

**12. DISTRIBUTION AVAILABILITY STATEMENT**

Public Availability

20010404 094

**13. SUPPLEMENTARY NOTES**

**14. ABSTRACT** In this work we have designed and synthesized high Tĝ yet ductile polymers using a building block approach. In this approach functional molecular groups that provide high Tg alternate with molecular linkages that provide mobility. Specifically molecular mobility is provided by in-chain cyclohexylene units. The existense of mobility is verified by dynamic mechanical studies, and supported by positronium annihilation studies. We discovered an unusual behavior in the three series of polymers studied wherein the higher mobility is found to be accompanied by higher Tg yet lower modulus. This observation is explained in terms of the increase in the persistence length of the polymer with increasing cyclohexylene ester content. The greater persistence length improves packing, resulting in higher Tg, while the mobility reduces interchain interaction, thus reducing modulus. This work suggests that the building block approach may allow scientists to synthesize polymers with various physical functions yet with ductility.

**15. SUBJECT TERMS**
polymers, termperature resistance; ductility; mechanical properties; glass transition

| 16. SECURITY CLASSIFICATION OF: | | | 17. LIMITATION OF ABSTRACT | 18. NUMBER OF PAGES | 19a. NAME OF RESPONSIBLE PERSON |
|---|---|---|---|---|---|
| a. REPORT | b. ABSTRACT | c. THIS PAGE | | | Albert F. Yee |
| U | U | U | UU | 73 | 19b. TELEPONE NUMBER (Include area code) (734) 764-4312 |

# A Rational Approach to the Design and Synthesis of Tough Glassy Polymers

Final Report December 23, 2000

U.S. Air Force Grant No. F49620-98-1-0158

Principle Investigator

Albert F. Yee

University of Michigan, Ann Arbor, Michigan

# 1 High Tg Polymers

In the last century, in the fields of materials, synthetic polymers have increasingly replaced classical materials such as wood, glass and metals.[1] In new material applications, polymers are now very often the materials of choice. Demand for increased performance in various areas such as military and electronic industries has led to significant advances in thermoplastics. High Tg, good mechanical properties, ready processibility, good optical and electrical properties have been greatly improved, but generally not at the same time. In the nineteen fifties, Shnell of Bayer AG and Fox of General Electric Co. synthesized the first polycarbonate with attractive thermoplastic properties. Its balance of key properties - excellent ductility, optical clarity, dimensional stability, Tg up to 148°C, and reasonable price-made it the engineering thermoplastic of choice for many purposes. However, there are requirements that this resin could not fill. Market demands for transparent plastics of higher Tg stimulated intense research and development in the 1960s. This led to the market introduction of polysulfones (PSO), polyethersulfones (PES), polyetherketones (PEK) and polyetherimide (PEI). These polymers exhibite good strength even at elevated temperatures. However their market share even today is limited due to their high cost and difficulties associated with their preparation. In some polymers with high melting points, increased crystallinity has rendered the polymers brittle, thus decreasing their suitability for many applications.

To increase Tg, generally bulky and rigid chemical units are incorporated into the polymer chain. This method is widely used. In his survey, Heijboer[2] pointed out that the introduction of stiff rings in the main chain is the most promising way for obtaining thermoplastics which are still stiff above 100°C, whereas a stiffening of the polymer by bulky side-groups (as e.g. in polyvinylcarbazole, Tg=210°C) is less promising, because such polymers are mostly brittle. As will be seen, in many cases both methods will result in very brittle polymers. For polycarbonate researchers, modification of the structures of polycarbonate is employed, with the objective of maintaining polymer chain's excellent properties, while gaining a significant increase in Tg. In tetramethyl bisphenol A polycarbonate, the bulky tetramethyl bisphenol A is used as the monomer, resulting in a polymer with Tg of 200°C; in polycarbonate of SBI, a rigid and bulky monomer SBI is used to give a polymer with Tg of 230°C. The structures of these two polymers are shown in Figure (1). But these polymers are extremely brittle at room temperature,[3,4] and efforts have been made to improve their ductility by copolymerization with bisphenol A, but with the sacrifice of Tg.

As pointed out recently by Primer and Feger,[5] high temperature polymers with a glass transition temperature greater than 150°C are key materials in the computer electronics industry. There are four major areas in the electronics industry that demand high temperature polymers: computer electronics, information storage, displays, and communications. These polymers must be ductile enough to meet the rigorous performance requirements. In other areas of applications, such as high Tg packaging materials and airplane canopy, both high Tg and good mechanical properties are required.

The general objective of the present study is to design and synthesize high Tg but ductile glassy polymers, specifically polyesters and polyestercarbonates. In order to achieve this, we need a molecular level understanding of how glass transition temperature, ductility and other mechanical properties are controlled, By the structure of the polymer on different length scales.

### 1.1 Glass Transition Temperature

In the past four decades, scientists have proposed theories or empirical correlations to predictthe dependence of Tg on molecular parameters. It has been generally recognized that intermolecular interaction (as indicated by cohesive energy density CED), intramolecular parameter (such as chain steric factor $\sigma$, characteristic ratio $C_\infty$ and persistence length $L_p$) and chain geometry play major roles in determining the glass transition temperature.[6-9] The correlations established so far have been successful in describing some types of polymers, but none has been successful in fitting polymers with aromatic groups in their backbones. The reason for this is difficult to pinpoint, but we believe that one key point is how to describe the stiffness of these polymer chains. For polyolefins and other simple polymers with carbon-oxygen backbones, $C_\infty$ and $\sigma$ are good molecular parameters to describe their chain stiffness. $C_\infty$ describes the stiffening by flexibility of bond angles and restricted rotation; while $\sigma$ indicates chain stiffening by restrictions to rotation. These two parameters fail to take into account chain stiffening by internal structures such as rigid cyclic rings, etc..[10] As put by Birshtein,[10] "A natural measure of flexibility is here only the absolute value, namely the length of Kuhn segment ..., or the persistence length." The concept of persistence length Lp was introduced long ago by Kratky and Porod[11] as a parameter for their wormlike chain model. This model is widely used for describing conformational characteristics of less flexible chains.[12,13]

### 1.2 Segmental Molecular Motion and Mechanical Properties

Main chain segmental molecular motions in polymer glasses play a crucial role in dictating their mechanical properties, such as yield stress, craze stress, and impact strength;[14-17] furthermore, it was proposed that these molecular motions can be enhanced by some types of conformational transitions in the main chain, such as the ring inversion of cyclohexylene group (C-ring).[15-18]

A correlation between the scale of molecular motion and yield stress was given by Chen and Yee,[15] and Liu and Yee.[17] Chen and Yee[15] studied structurally similar polyesters and Liu and Yee[17] studied structurally similar polyestercarbonates. They observed that as the activation volume increased, the yield stress dropped. The increased activation volume was interpreted as an increase in the scale of polymer chain motions, which could relax stress more effectively, thus facilitating the yielding process. A more direct correlation between the scale of molecular motion and yielding process was given by Xiao et al.[14]. By systematic chemical modification of their polymer structures, they tailored the scale of molecular motion as probed by DMA. They found that when the scale of in-chain cooperative motion was small, a higher temperature was needed to activate yield in the copolymer; when the scale was large, the brittle to ductile transition temperature shifted to a much lower temperature.

Phenomenologically yielding is temperature and rate dependent and can be described as a non-linear stress relaxation process. However, in spite of extensive research activities in this area,

there is still no general consensus on the molecular mechanism of the yielding process. Different molecular models have been proposed to explain the yielding process. These include Eyring's transition state model,[19] Robertson's conformational change model,[20] Argon's disclination model,[21] and others. A detailed review of molecular models on yielding was given by Crist[22] and Stachurski.[23] All the models enjoy more or less success in explaining and fitting experimental results. Among these, the Eyring model is the most general and the most successful, but it lacks molecular detail. Robertson's model is intramolecular in nature, whereas Argon's model is intermolecular in nature.

The understanding of the effect of molecular motion on intramolecular interaction and intermolecular interaction is crucial before we can derive a better molecular model.

## 2 Approach and Experimental

A building-block approach is used to obtain high Tg and ductile polymers. In this approach, some molecular units are used to provide high Tg or other functions, while other units are used to introduce cooperative segmental motions. For this approach to work the motion of the latter units must couple with the former units via suitable linkages. In this work ester linkages are used. Three bisphenol monomers are used(Figure (2)). SBI differs significantly from bisphenol A in structure. SBI is rigid and bulky, it does not have much mobility; 4,4'-(3,3,5-Trimethylcyclohexylidene)diphenol (Tmc) has a very rigid and bulky side chain C-ring, which does not undergo ring inversion; but for 4,4'-cyclohexylidenebisphenol (BPAZ), the side chain C-ring undergoes facile ring inversion. SBI and Tmc are used to make high Tg polymers. By incorporating main chain C-rings, we hope to enhance the mobility of SBI and Tmc and get enhanced ductility. In this way, BPAZ is used to make polymers with not only mobile side chain C-rings but also main chain C-rings. This allows us to see whether there is a difference in the effect of motions of side chain C-rings from that of main chain C-rings on physical and mechanical properties.

Polycarbonates, polyesters, and poly(ester carbonates) were made using the solution condensation technique. The chemical structures are shown in Figure (3). Tg and molecular weight are shown in Table (1). In this work, DMA was used to get secondary relaxation and thermal expansion data. DSC was used to obtain Tg. An Instron testing machine was used to conduct tensile tests at 24°C to get Young's modulus, yield stress, necking and post-yield stress drop information. Positron annihilation lifetime spectroscopy (PALS) was used to provide information on chain packing in the glasses and thermal expansion of nanosized holes.

## 3 Results and Discussion

### 3.1 γ Relaxation

#### 3.1.1 sub-Tg γ Relaxation of Polymers Based on SBI

The fact that SBI-PC has a γ relaxation similar to that of BPA-PC was reported by Stueben[3] three decades ago. Even though the peak position and intensity are essentially identical to those

of BPA-PC, the polycarbonate was found extremely brittle. The brittleness of this polymer would not be surprising if we consider the chemical structure of SBI. In SBI, the central linkage between the phenyl rings consists of two spiro-linked five-membered rings, which are fused to the phenyl rings at the para and meta positions to the oxygen atom. The SBI moiety is bulky and locked in a twisted conformation. The phenyl rings cannot rotate unless the entire moiety moves as a unit, which is probably difficult in the glass. The γ relaxation of this polymer was also reported by Pessan et al.,[24] and studied by Wimberger-Friedl and Schoo[25] in more detail. They concluded that the phenyl motion was not required for the typical γ relaxation of polycarbonate at low temperature, and the relaxation was due to the motion of the carbonate group. The DMA spectra for SBI-PC are reproduced from the work of Pessan et al.[24] and Wimberger-Friedl[25] in Figure (4). Also in the figure is plotted the spectrum of BPA-PC from our own work. Considering that the spectra are from different groups obtained with different instruments, we cannot elaborate on these spectra beyond saying that SBI-PC does have a γ relaxation similar in peak shape and peak position to those of BPA-PC. Our previous work on BPA-PC suggests that several repeat units are involved in the γ–motion.[14]

There are two possible motions to relate with the sub-Tg γ–relaxation of SBI-PC. One is the motion of the carbonyl group; the other one is the cooperative motion in which SBI moves along with the carbonate group as a rigid body. The exact nature of this motion is the subject of this investigation.

The incorporation of C-rings into a polymer backbone changes itsDMA spectra drastically. Shown in Figure (5) are the DMA spectra for SBI-PC, SB, BPA-PC, SC, and SCBC. At around -70°C, a prominent peak appears in SC and SCBC; the peak typical of polycarbonate for SBI-PC, SB, and BPA-PC at around -100°C has disapppeared in these two polymers. The new peak at -70°C is very similar to that of PCT[18] both in shape and peak position. Since the introduction of ester groups into BPA-PC does not change the relaxation behavior at all,[26] the new peak at -70°C cannot be due to the ester group alone. So the most probable motion is that of C-ring inversion, which quite possibly cooperates with its neighboring ester groups. SCBC can introduce complexity in motion modes by having BPA moieties on its chain, but its DMA spectrum is basically the same as that of SC. The similarity in DMA spectra among these polymers and their similarity to that of PCT indicates that all of them involve C-ring motion, and most probably the ring inversion. This conclusion will be further substantiatedin the following sections.

#### 3.1.2 γ Relaxation of Polymers Based on BPAZ

The DMA spectrum of ZPC does not follow the general observation that replacement of isopropylidene group in BPA-PC will not change the DMA spectrum of corresponding polycarbonate as reviewed by Yee and Smith.[27] Replacement of the isopropylidene group by a cyclohexyl group shifts the γ relaxation peak up nearly 40°C at 10 Hz(Figure (6)). This up shift was reported by McHattie et al.[28] and by Hörth et al.[29]. McHattie et al. did not offer an explanation for the origin of this relaxation, but stated that the flexible cyclohexyl ring improved the chain packing, and resulted in smaller free volume than that of BPA-PC, therefore the relaxation occurred at a higher temperature. This free volume explanation has two shortcomings. Firstly, free volume cannot explain the up-shift of nearly 150°C at 1 Hz of tetramethly bisphenol-A polycarbonate compared with that of BPA-PC,[27] even though the free volume for the former

is largerthan that of the latter;[30] secondly, a different method of assessment may result in a different value of free volume. The occupied volume at 0 K needs to be estimated in order to calculate the free volume, but different estimation methods such as those of Sugden and of Bondi give quite different results,[28] which makes the free volume interpretation ambiguous.

Zhao et al.[31] conducted solution and solid state NMR studies on the dynamics of ZPC. In solution they observed that the C-rings undergo rapid ring inversion with an activation energy of 28 kJ/mole and correlation time prefactor of 6.5 _ $10^{-11}$s. But in solid they did not find the ring inversion in the chemical shift time scale over the temperature range of -100°C to 100°C, which means if the ring inversion does occur, its rate is slower than kHz. In the solution state at low-temperature and in the solid state, the two phenyl rings are not equivalent as they observed. The axial phenyl ring is much more restricted in motion than the equatorial ring, and based on the line shape analysis of the bridge carbon linking the two phenyl rings, an activation energy of 53.9 kJ/mole for the relaxation was calculated. Based on these results, they proposed that the up shift of the γ relaxation peak is due to the more restricted motion of the axial phenyl ring. This explanation is plausible, but may not be the main reason, if we consider other structures.

In TmcPC, there exists severe steric interaction between the axial phenyl ring and the axial methyl group as evidenced by NMR. This is also true in the polycarbonate of norbornyl bisphenol (NBPC)(Figure (7)). But TmcPC has a γ relaxation peak very similar to that of BPA-PC. This will be shown later in the discussion on the relaxation of Tmc polymers. NBPC was also shown to have a similar relaxation peak to that of BPA-PC.[28] Obviously, the restricted rotation of phenyl ring alone cannot explain the large up-shift in the γ relaxation of ZPC.

The relaxation peak at around -50°C at 10 Hz for ZPC is actually typical of the relaxation involving C-ring inversion. This implies that the up-shifted and broad relaxation peak in ZPC is dominated by C-ring inversion. Compared with SC, ZPC is much broader on the high-temperature side, which may be due to the stronger coupling between the C-ring and the backbone units as evidenced by the steric interaction between the C-ring and the axial phenyl rings from NMR results. In SC, since the rigid SBI moiety may not transmit motion down the chain effectively, the C-ring motion is most likely very localized, resulting in a narrower relaxation peak.

The incorporation of increasing amounts of C-rings into the polymer backbone does not change drastically the shape and position of the γ relaxation peak in ZPC; unlike in SBI-PC(Figure (8)), the peak shapes and peak positions remain the same. With increase in main chain C-ring content from ZPC to $Z_1C$, the damping peak intensity increases and the drop in storage modulus (relaxation strength) also increases. The change in the damping peak intensity with the change in main chain C-ring content prompts us to conclude that in $Z_xC$ polymers their γ relaxations involve main chain C-rings. The similarities in peak position and peak shapes indicate that the relaxation mechanism it represents is the same in ZPC, ZCBC and $Z_xC$, and involve C-rings. In ZPC it involves side chain C-rings; while in $Z_xC$ it involves both side chain and main chain C-rings. The similarity in the effects of the motions of side chain and main chain C-rings on the relaxation spectra is not surprising, since they involve similar conformational changes, the only difference being the degree of their coupling with their neighbors. The degree of this coupling is

difficult to determine, but may be inferred from changes in other properties with the change in C-ring content. In describing the DMA damping peak intensity for ZPC, ZCBC and $Z_xC$, we need now consider not only changes in main chain and side chain C-ring concentrations, but also the total C-ring concentration. This may explain why ZCBC has a lower peak intensity than $Z_1C$: despite its having the largest main chain C-ring content, its total C-ring concentration is smaller. This will be elaborated on later in a quantitative discussion of the correlation between relaxation strength and total C-ring concentration.

An activation energy of 56.14 kJ/mole, and prefactor of $6 \_ 10^{13}s^{-1}$ are calculated for the $\gamma$ relaxation of ZPC according to the peak position and its corresponding frequency. At room temperature and 100°C, the ring inversion frequency should be around 10 kHz and 85 kHz respectively. Now let us ask this question: if the $\gamma$ relaxation in ZPC is due to the C-ring inversion, why did the solid state NMR by Zhao et al. not show the inversion on the ms scale? There are two possible ways to explain this apparent discrepancy. Firstly, the frequencies calculated according to the activation energy and prefactor are only for the peak position. In fact the relaxation peak is very broad, and covers a range from around -110°C to 50°C. At a given frequency and temperature, some relaxations may be activated, but some may not. Secondly, the solid state NMR spectrum by Zhao et al. has very broad peaks, as shown in Figure (9). The resonance at 143 ppm is the 4e carbon (the labeling is shown in Figure (10)), and the 4a carbon is obscured by the C1 resonance at 150 ppm. The collapsed signal for C4 due to rapid ring inversion should be around 147 ppm according to their solution NMR results, but this is also obscured by the C1 resonance. So it is very possible that some C-rings do undergo rapid ring inversion, but theirsignal is obscured by the broad line width. We believe the DMA results in the related polymers containing C-rings are quite unambiguous, while the broad line NMR results are not incontrovertible.

#### 3.1.3 $\gamma$ Relaxation of Polymers Based on Tmc

The TmcPC peak is much narrower and has a smaller peak intensity than that of the $\gamma$ peak in BPA-PC; also the peak position is around 10°C lower than that in BPA-PC at 10 Hz(Figure (11)). NMR shows that the bulky side chain C-rings on TmcPC are locked in their chair forms. There is severe steric interaction between the axial phenyl rings and the axial methyl groups. Solution 13C-NMR study[32] showed that the axial phenyl ring has a much more restricted motion with an activation energy of about 41.8 kJ/mole, while the equatorial phenyl ring has a much freer rotation with an activation energy of less than 12.54 kJ/mole. The 41.8 kJ/mole rotational activation energy is much larger than that in BPA-PC in solution, which is around 12.54 kJ/mole.[33] We think this restricted motion of the axial phenyl ring may account for the narrowing of the peak on the high-temperature side. This can be corroborated by the result in SB polymer. The phenyl rings in the SBI moiety do not have the ability to rotate. The relaxation peak, as shown in Figure (11), is also much narrower than that in BPA-PC. Also, the $\gamma$ relaxation peaks of SB and TmcPC are strikingly similar. This phenomenon was also observed by Wimberger-Friedl and Schoo[25] in their DMA study of copolycarbonates of SBI and BPA. As shown in Figure (12), with the increase in BPA content in the copolymer, the higher temperature side of the DMA curve is broadened systematically. The authors attributed this broadening to the contribution of BPA's motion, specifically, the phenyl ring motions.

Figure (13) shows the γ relaxation peaks of TmcPC, the copolymers $Tmc_xC$, and TmcCBC. As with main chain C-ring incorporation in SBI polymers, the γ relaxation behavior of these polymers changes dramatically. The peak of TmcPC has disappeared, and a new peak typical of relaxations with C-ring inversion emerges at a higher temperature in $Tmc_xC$ and TmcCBC. In $Tmc_5C$ and $Tmc_3C$, the peaks are more asymmetric with a trace of the relaxation of TmcPC on the lower temperature side. With the increase in C-ring content, the damping peak intensity also increases and the peak broadens. This change in intensity with C-ring content can be due to two reasons. First, the C-ring incorporation enhances molecular motion; second, there is a concentration effect. In order to understand this and also explain a similar question in polymers based on BPAZ, we will discuss the γ relaxation quantitatively in terms of its relaxation strength.

Through the results and discussions of the dynamical mechanical behavior of polymers based on SBI, Tmc and BPAZ, we can conclude that the relaxation peak at around -50°C at 10 Hz is due to the C-ring inversion.

#### 3.1.4 Relaxation Strength

A suitable quantitative parameter for describing the γ relaxation, besides the peak position and activation energy, is the relaxation strength. In DMA the relaxation strength is indicated by the effect of a molecular motion on the modulus. It is defined as:

$$\Delta E' = E_u' - E_r' \qquad (1)$$

where $E_u'$ stands for the "unrelaxaed" modulus, that is, the modulus determined at a much higher frequency than that of the relaxation process, and $E_r'$ stands for the"relaxed" modulus, that is, the modulus determined as a frequency much lower than that of the relaxation process. As pointed out by Heijboer,[34] it is very difficult to determine the relaxation strength experimently. The difference between E' values far apart on the frequency scale usually cannot be determined with sufficient accuracy, since each value has to be determined by a different technique. Therefore, he recommended determining relaxation strength from a E' vs T curve instead of from a E' vs frequency curve. $\Delta E'$ can then be determined in the way indicated in Figure (14).

As shown in Figure (15), there is a nice linear correlation between the relaxation strength and the mole concentration of C-rings. The latter refers only to main chain C-rings for polymers based on SBI and Tmc, since they do not have side chain C-rings; whereas for polymers based on BPAZ, it refers to the total concentration including both main chain and side chain C-rings. This linear correlation indicates that there is no difference, at least in relaxation strength, between the side chain C-ring and main chain C-ring. As we have discussed, since the side chain C-ring on the BPAZ moiety couples strongly with the backbone phenyl rings, we would expect that the main chain C-rings should have the same or stronger coupling with their neighbors, but the degree of coupling cannot be determined by the DMA results so far obtained.

Heijboer[34] studied the mechanical relaxation due to the chair-chair transition of cyclohexyl rings as side groups on polymer chains or as part(s) of plasticizer molecules in different polymeric matrices. His work shows that the relaxation strength $\Delta G'$ is simply proportional to the number

of C-ring groups per unit volume (see Figure (16)) and independent of the local environment of the group. It does not matter whether the C-ring is part of a plasticizer molecule or part of the side chain in a plasticized or non-plasticized polymer. Even though, in both Heijboer's system and ours, there is a linear correlation between the relaxation strength and the C-ring concentration, the value of relaxation strength per mole/L of C-rings is different. We cannot compare them directly, since Heijboer used $\Delta G'$ and we use $\Delta E'$. However, approximately $\Delta E' = 2\Delta G'(1+\mu)$. Since Poisson's ratio $\mu$ ranges for most polymers from 0.3 to 0.45, we can convert the $\Delta G'$ into $\Delta E'$ in Heijboer's result by assuming $\mu$ as 0.38. Thus, $\Delta E'$ is around 261 MPa per mole/L for Heijboer's polymers, which is much smaller than 338 MPa per mole/L of our polymers. This difference is significant enough not to be introduced by the conversion, which should be around 20 MPa per mole/L at most. However, relaxation strength is related with $\Delta U_0$, the conformational energy difference between one chair form and the other one after ring inversion.[34,35] The smaller $\Delta U_0$ is, the larger the relaxation strength. The C-rings in Figure (16) have $\Delta U_0 = 0.7$ kcal/mole, and for C-rings with $\Delta U_0 = 0$, $\Delta G'$ is 113 MPa per mole/L,[35] which after conversion into $\Delta E'$ is around 312 MPa per mole/L, agreeing favorably well with 338 MPa per mole/L of our polymers. Since $\Delta U_0$ of C-rings in BPAZ is 0 kcal/mole, and those in main chain C-rings are around 2.2-2.4 kcal/mole,* they may have different relaxation strengths, but the difference is within experimental error.

## 3.2 Thermal Expansion and Glass Transition

### 3.2.1 Thermal Expansion

Almost all solids expand on heating. Except for phase transitions, thermal expansion in solids is a result of the anharmonicity of lattice vibrations. Materials with covalent bonds such as diamond, silicon and silica have very low expansion coefficients, roughly 100 times smaller than those of polymers;[37] this is because these covalent bonds have very low anharmonicity. On the other hand, the coefficients of thermal expansion of polymers are the summation of those along the chain and those among the chains. Since polymer chains are very anisotropic, the expansion coefficient is very different along the chain from that between the chains. Along the chain, strong covalent bonds produce very small thermal expansion; between polymer chains, however, the much weaker van der Waals force binds polymer chains together. The higher anharmonicity results in larger thermal expansion. Thus the contribution toward the total thermal expansion coefficient from that along the chain is negligible, and the thermal expansion of a polymer is basically an expansion of the distance among polymer chains. This point was well recognized by previous researchers.[23,38-42] For polymers, as stated by Stachurshi,[23] "a 3-dimensional macroscopic volume expansion is always derived from 2-dimensional expansion orthogonal to the chain axis."

---

* Estimated by assuming an equatorial ester group is favored by 1.1-1.2 kcal/mole over an axial one.[36]

LCTE values in the temperature range of -120°C to 100°C are shown in Figures (17, 18, 19).

Figure (17) shows that SC and SCBC have very similar thermal expansion coefficients within the temperature range studied. For both the Tmc and BPAZ series, with the increase in main chain C-ring incorporation, the LCTE increases. We have shown that there is a linear correlation between the relaxation strength and the total C-ring concentration. It is important to see whether such a correlation can be established in terms of LCTE. Shown in Figure (20) is the plot of LCTE of BPAZ polymers at 24°C versus the total concentration of C-rings. Obviously, the LCTE value for ZCBC makes the correlation invalid; ZCBC has the greatest LCTE, but its total C-ring concentration is not the greatest. This may hint at a major contribution from BPA units on the thermal expansion, but the following discussion, suggests that it is not the case.

As seen in Figure (21), there is a good linear correlation between LCTE and main chain C-ring concentration for both the Tmc and BPAZ polymers. Upon replacement of half of the Tmc monomers by BPA monomers in $Tmc_1C$, TmcCBC is obtained; but this replacement does not cause the LCTE of TmcCBC to deviate from the linear line to any significant degree, and this is also the case in ZCBC. This observation makes it clear that the non-existence of correlation between LCTE and total C-ring content is not due to the replacement of BPAZ with BPA. As we have discussed, LCTE is predominantly a result of interchain interactions. The increase in LCTE with the content of main chain C-ring instead of that of total C-ring indicates two things. First, main chain C-ring incorporation decreases interchain forces; second, main chain C-ring motion can modify the interchain interaction more effectively. We propose that the motions from intrachain segments can reduce the surface contact area and the contact time between polymer chains, thus weakening interchain interaction. The inversion of main chain C-rings may introduce large scale and fast segmental motions, which should be more effective in modifying the interchain potentials. We suggest that due to the chair-chair inversion of these main chain C-rings, the local motional mode may be altered, and to some extent, cooperative motions with their neighbors may be involved. Whereas side chain C-ring motion will be less effective in activating its main chain neighbors, since only one end of the ring is anchored to the polymer chain.

Figure (22) can help us to visualize the effect of main chain C-ring inversion on its neighbors. In this figure, a trans C-ring is linked to two bulky and rigid SBI entities. When the C-ring undergoes inversion from the top chair to the bottom chair through a twisted boat configuration in the middle, there must be by necessity a larger spatial reorientation of its neighbors. The picture may be too idealistic; in reality this reorientation may require the cooperation of nearby C-rings.

Figure (21) shows that even though the change in LCTE is mainly a result of the main chain C-ring incorporation, the absolute values of LCTE are higher for the BPAZ series than those of the Tmc series. This may indicate different contributions from other units. The Tmc moiety is less mobile than the BPAZ moiety. In Tmc, the side chain C-ring is locked into a chair form, the axial phenyl ring undergoes restricted rotation; whereas in BPAZ, the side chain C-ring undergoes rapid ring inversion, and the phenyl ring rotation is more free. Thus motions in the BPAZ entity can be activated more easily than those of the Tmc unit at the same temperature, therefore motions from BPAZ weakens interchain forces more effectively than Tmc does. The

LCTE values of both SC and SCBC fall close to the line of BPAZ series and are higher than the corresponding Tmc counterparts, even though the SBI moiety is less mobile than either BPAZ or Tmc. Also within the entire temperature range studied, the LCTE values for SC and SCBC are almost exactly the same. As will be discussed in the next section, the bulk CTE values are "apparent" ones which could give an incorrect relationship, and the "real" relative order of CTE values of these polymers will be laid bare in discussing the thermal expansion of nanosized holes probed by PALS.

**3.2.2 Coefficient of Thermal Expansion of Nanosized Holes**

In the expression for bulk CTE, $\alpha = \frac{dV}{VdT}$. dV , the volume change, is predominantly due to the expansion of interchain space, while V is comprised of both the interchain space and van der Waals volume. So bulk CTE is an "apparent" value and is reduced to roughly one order of magnitude smaller than those of the unoccupied volume. The CTE of the unoccupied volume is a direct measure of chain mobility, through which the effect of main chain C-ring incorporation on chain dynamics could be seen more clearly. The unoccupied volume can be measured by PALS.

The change in $\tau_3$ with temperature is shown in Figure (23) for $Tmc_5C$. $\tau_3$ increases with temperature from -140°C up to 100°C. Above 100°C, the increase in $\tau_3$ with temperature slows down This behavior is typical of the series of polymers. The exact reason is not clear. We speculate that it could be because the γ-relaxation contribution is saturated at temperatures higher than 100 °C. In most cases, the γ relaxation involving C-ring inversion can be detected as the one shown in Figure (23). The rate of the change in $\tau_3$ with temperature increases abruptly around the γ relaxation temperature, $T_\gamma$.

In Figures (24, 25, 26) are shown the changes in the lifetime of o-Ps with temperature for the polymers of the SBI series, Tmc series and BPAZ series. A common feature of all these polymers is that before the secondary relaxation takes place, the average hole sizes decreases with the increase in main chain C-ring content, which is especially pronounced on the lower temperature side; but after the γ relaxation takes place, the rate of hole size expansion increases with the increase in main chain C-ring content, which inverses completely or partial by the trend of the hole sizes on the lower temperature side.

At very low temperatures, especially when the temperature approaches 0 K, the interchain space due to inefficient chain packing contributes most to the total hole size. Consequently the relative order of hole sizes indicates the packing efficiency of different polymers. As temperature increases, especially with the onset of the γ relaxation, the contribution toward the total hole size from the dynamic interchain expansion becomes larger and larger. After a certain point, the contributions from the γ-relaxation changes the relative order of hole sizes. Chain packing efficiency is mainly determined by two factors, namely, chain topology and chain dynamics. A streamline-shaped polymer chain is conducive to efficient chain packing, while chain dynamics provides the mobility for the packing process, with which the polymer chains can adjust themselves to the lowest energy arrangement permitted by the time scale. As will be discussed in the next section, trans- main chain C-rings will provide the polymer chain with a more extended

configuration, which is beneficial to chain packing. At the same time, the chain dynamics enhanced by the main chain C-ring inversion will help polymer chains achieve a lower energy state when they change from the melt state toward the glassy state.

The parameter quantitatively related to the chain dynamics is the coefficient of thermal expansion of nanosized holes. Since the change in hole size with temperature is not as smooth as in the case of bulk dimensional change, a second order polynominal cannot give a reasonable fit. In this part, we will not try to calculate the CTE of open holes at all temperatures; instead, we will only look at the values at 24°C, a temperature at which all the mechanical tests are done. Shown in Figures (27, 28) are the hole CTE of all the polymers. The bulk coefficients of thermal expansion of SC and SCBC are almost exactly the same within the temperature range of -120°C to 100°C, but the nanosized hole CTE of SCBC is apparently greater than that of SC at room temperature and is the largest among SC, SB and SCBC. As we mentioned, bulk CTE is an "apparent" value, since it is reduced by the van der Waals volume, which contributes negligibly to the volume expansion. So the hole CTE is a real indication of chain dynamics. The chain distance estimated from the hole size is much larger for SC than for SCBC, and this factor should reduce the interchain force more in SC. But the overall interchain force is smaller for SCBC judging from its greater hole CTE value; and this, we propose, is due to the more enhanced intrachain dynamics in SCBC. In SCBC, there is a possible cooperative segmental motion in each CBC segment,[16] which can effectively affect the interchain interaction by reducing the contact surface area and contact time, thus reducing interchain force. The scale of this kind of segmental motion is much curtailed in SC, since the segmental motion may be stopped at SBI sites due to its bulkiness., This point will become clearer in discussing their mechanical behavior.

As shown in Figure (28). with the increase in main chain C-ring content, the CTE of nanosized holes in Tmc polymers and BPAZ polymers increases accordingly. The absolute values of the CTE of BPAZ polymers are greater than those of their Tmc counterparts. This is due to the same reason as discussed in the bulk CTE case. SC, SCBC fall in the family of Tmc polymers, different from what we observed in bulk CTE results, in which SC and SCBC fall in the family of BPAZ polymers instead. The relative order of the CTE values should be made according to hole CTE values instead of bulk CTE ones, since the latter are "apparent" numbers. Polymers made from SBI are more akin to Tmc counterparts: SBI and Tmc have the same molecular weight, and their structures are both rigid and bulky, their polymers have similar Tgs, and, as will be shown, SCBC and TmcCBC even have similar mechanical properties. So CTE values of nanosized holes illiminate the real relationship which is obscured by bulk CTE ones.

#### 3.2.3 Glass Transition Temperatures

Up to this point, we have shown that the secondary relaxation strength increases with the increase in the total C-ring mole concentration, and thermal expansion coefficient increases with the increase in the main chain C-ring incorporation. Figure (29) shows that Tg also increases with the increase in the main chain C-ring content. In this section, we will show that persistence length is the predominant factor controlling Tg.

As we have discussed in the introduction part, various correlations between Tg and molecular

parameters fail to include polymers with main chain aromatic groups. This may be because the parameters $C_x$ and $\sigma$ cannot describe chain stiffness correctly for these polymers. On the other hand, persistence length $L_p$ or Kuhn length is the natural measure of chain stiffness. The calculation of persistence length is not a trivial matter, it demands detailed knowledge of polymer chain energetics. However, the increase in Tg with $L_p$ has been shown experimentally.[43,44] In another case, the partial substitution of the carbonate units in polycarbonate by terephthalate groups leads to a systematic increase in Tg. Qualitatively, this has been ascribed to the increase in persistence length.[45,46] Upon the replacement of up to 50% of the carbonate groups in BPA-PC by terephthalate groups, the Tg was increased from 150°C to 192°C. From Figure (30), we can see qualitatively that the replacement of carbonate groups by terephthalate groups can lead to increased persistence length. In BPA-PC, the carbonate groups can take either trans- or cis- conformations. The cis- conformation introduces a kink into the polymer chain, which reduces the persistence length. The incorporation of terephthalate groups can delay this kink formation by at least the length of this rigid group, thus increasing Lp.

A trans- C-ring has a close resemblance in shape to that of a phenyl ring. The incorporation of trans C-rings should therefore have the same function as that of phenyl groups to extend polymer chains. This can be seen clearly in Figure (31) for Tmc polymers. The results of Wu, and Liu[26,47] further substantiate our proposal. In $B_xt$ polymers, terephthalate groups (t) were periodically inserted into polycarbonate of BPA, where x was the number of repeating units in each polycarbonate block; in $B_xC$, instead of terephthalate groups, cyclohexylene dicarboxylate groups were inserted into BPA-PC. From Figure (32), we can see that the two series of polymers have almost the same Tg at the same mole fraction of terephthalate groups or main chain C-ring groups. Thus trans main chain C-rings, like phenyl rings, extend the polymer chain, resulting in increased persistence length, and therefore increased Tg.

Now we have to answer a crucial question: why do our polymers behave so differently than other traditional polymers in that both our glass transition temperature and thermal expansion coefficient increase at the same time? We have discussed in the thermal expansion section that the incorporation of main chain C-rings weakens intermolecular forces which will work against enhancing Tg from the cohesive energy density point of view. This leads to our conclusion that the increase in Tg with increase in the main chain C-ring content is mainly due to the stiffening of polymer chains by these C-rings. However it is important to note that "stiffening" refers only to increase $L_p$.

The main chain C-ring undergoes rapid inversion even at room temperature; at Tg, these inversions are even faster. After an inversion, a trans- C-ring with two equatorial substituents becomes a trans C-ring with two axial substituents, introducing a step instead of a kink into the polymer chain. As shown in Figure (33), this step only slightly reduces the stiff segment length. Furthermore, the conformational free energy for an ester group is around 1.1-1.2 kcal/mole.[36] Since there are two ester groups on a main chain C-ring, the equatorial-equatorial trans C-ring is favored in energy by about 2.2-2.4 kcal/mole, which indicates that at least 90% of the trans C-rings are in the equatorial-equatorial conformation. So the trans- C-ring plays the role of stiffening polymer chains. By contrast, a cis- C-ring has one substitutent at the equatorial position, and another one at the axial position, thus cis- C-rings introduce kinks into the polymer

chain, significantly reducing the length of the stiff segment. Consequently we expect a great deal of decrease in glass transition.

This analysis is supported by the data in Table (2). Polymers based on SBI with the same chemical structure but with different C-ring configurations show drastically different Tgs. Polymers with C-rings of cis:trans=72:28 have glass transition temperatures at least 40°C lower than their trans counterparts.

## 3.3 Mechanical Properties

### 3.3.1 Yielding

SBI-PC is extremely brittle.[3] By incorporating main chain C-rings, we hope to induce enough chain motion to make the polymers yield. But the polymers with C-ring mole fraction up to 0.5 fail to behave ductilely. We know in Figure (34) the tensile behavior of SC, SB and SCBC. Both SC and SB fail in a brittle manner, while SCBC fails in a ductile manner. In a previous section we have showedthat the C-ring inversion is still active in SC; from its brittleness, we deduce that the inversion of C-rings may not be sufficient to activate its bulky SBI neighbor ; i.e., the polymer chain motion is still very localized. The motions from the carbonate group, the BPA moiety and/or the combination of these two entities fail similarly to give enough motivation to SBI. This may be the reason why SB behaves in a brittle manner. Interestingly, SCBC undergoes plastic deformation at different strain rates ranging from $8.4 \_ 10^{-4}\ s^{-1}$ to $4.3 \_ 10^{-2}\ s^{-1}$, as shown in Figure (35). In a single chain of SCBC, between every two SBI moieties, there is, on average, a CBC segment . From DMA results, we know that the characteristic C-ring inversion is active in SCBC. Apparently this motion provides the final step for the chains to flow past each other at larger strains. While the molecular mechanism is still not completely clear, by comparison with SC and SB, where a single C-ring unit or a BPA unit alone can not help the polymer to yield, we can infer that the CBC segmental motion plays a crucial role in facilitating the plastic deformation.

Figures (36) and (37) show the tensile behavior of polymers based on Tmc and BPAZ. Both figures show that with the increase in main chain C-ring content, yield stress drops. This behavior is seen more clearly in Figure (38). Also, with the increase in main chain C-ring concentration, Young's modulus drops, as shown in Figure (39). Interestingly, the plot of yield stress/Young's modulus versus total C-ring concentration in Figure (40) shows no correlation. This suggests that the change in this ratio is mainly determined by the change in main chain C-ring content, not by side chain C-rings. This observation is similar to that of the thermal expansion change, and obviously different from that of the secondary relaxation strength. The similarity in response between thermal expansion, yield stress, and Young's modulus to the change in main chain C-ring concentration suggests that they have similar molecular origins.

### 3.3.2 Yield Stress and Young's Modulus

Figure (41) shows that there is a linear correlation between Young's modulus and the inverse of linear thermal expansion coefficient at 24°C for all the polymers we have studied. Interestingly, there is also a near linear correlation between yield stress and the inverse of LCTE as shown in Figures (42) and (43). These correlations imply that there should be a near linear correlation

between yield stress and Young's modulus, which is indeed observed in Figure (44).

As discussed previously, thermal expansion is mainly the expansion of the distance between polymer chains. The near linear correlation between Young's modulus and yield stress suggests that interchain interaction also dominates the yielding process. In this sense, this phenomenon is in accord with Argon's model for plastic demormation.[21] In his model, the plastic deformation is modeled as an activation process overcoming intermolecular interactions. Yang found, in her molecular dynamic simulation of the deformation of amorphous polyethylene, that the strain energy from Lennard-Jones potential dominated the total strain energy as shown in Figure (45).[49] A similar result was observed by Fan in his molecular mechanics study of the yielding of glassy polycarbonate.[50] The maximum of the derivative of total strain energy with strain gives the yield stress, therefore in this sense, yield stress is also governed mainly by interchain interaction. The linear correlation between Young's modulus and yield stress was reported by many researchers.[51-53] This observation may lead to the conclusion that interchain interaction is the sole factor controlling yielding process. Numerically this seems to be correct, but stating so under-estimates the effect of intrachain interaction on interchain forces. As discussed previously, the incorporation of main chain C-rings in our polymers leads to enhanced in-chain segmental motion. These motions, especially the fast flip-flop motion of main chain C-rings, apparently modify the interchain interaction through decreasing the effective contact areas and interacting times, and as a result, the intrachain motion modulates the interchain interaction. This modulating effect is most effective through main chain segmental motion as demonstrated in the good correlation between LCTE, yield stress/Young's modulus and the main chain C-ring concentration instead of total C-ring concentration (including side chain C-rings).

#### 3.3.3 Activation Volume and Post-yield Stress Drop

The log strain rate dependence of yield stress at room temperature for all the polymers studied in this work follows well the Eyring equation as shown in Figures (46, 47, 48). From the slope of the yield stress vs. strain rate plot, we can calculate the activation volume for the yielding process. Figures (49) and (50) show that in both Tmc and BPAZ polymers, the Eyring flow volume increases with the increase in main chain C-ring concentration. This means more molecular segments are involved in the yielding process as more main chain C-rings are incorporated. As discussed in a previous section, the main chain C-ring inversion may require large scale reorientation of its neighbors Apparently this cooperative motion is more effective in dispersing strain energy. The more such motion exists in the system, the easier the local stress can be relieved by sharing with other polymer chains. SBI has the same molecular weight as Tmc, but the former is severely restricted in the freedom of motion because of its locked configuration, while the latter has restricted motion due to steric interaction between axial phenyl group and the axial methyl group. Interestingly, TmcCBC and SCBC have basically the same Tg, very similar LCTE and mechanical properties. Figure (49) shows that SCBC has a similar activation volume to that of TmcCBC. This, in a sense, is remarkable because in the external thermal/stress field, TmcCBC and SCBC respond similarly despite their inherent difference in small strain mobility. This suggests that in SCBC, SBI has very similar mobility to that of Tmc, and SBI is activated into motion by the cooperative motion of CBC segment. We note that yield occurs at large strains and it is possible for the large strain to enhance segmental activity.

In most engineering stress versus engineering strain plots for ductile polymers, a post yield stress drop (PYSD) is observed as shown in Figure (51). This stress drop is called strain softening and is usually accompanied by necking in a tensile test. Brown and Ward found that in most cases there was clear evidence for the existence of an intrinsic yield drop, i.e. a fall in true stress.[54]

As shown in Figures (36, 37), all the polymers show PYSD except $Z_1C$ and ZCBC. It is hardly noticeable for $Tmc_1C$ and TmcCBC. Except for $Z_1C$, ZCBC, $Tmc_1C$ and TmcCBC, all other polymers show obvious necking. We are interested in why some polymers tend to have necking, and others not.

Necking is closely related with stress/strain localization In uniform deformation, this strain localization is insignificant. The tendency of glassy polymers to undergo localized plastic deformation (necking) or diffuse one was correlated with the "natural hinge length" $\bar{l}$ of a group of polyimides by Argon and Bessonov.[55] The chemical structures and physical properties of the glassy polyimides they studied and some other polymers are listed in Figure (52). $a_0$ is the molecular radius determined from crystallographic data. It describes the width of the molecule; $\bar{l}$ is the spacing of natural 'hinges' on molecules, i.e. the lengths of the stiff units (segments) in the polymer chains. For the four polyimides, they observed that as the natural hinge length increased, the tendency to necking was decreased (Figure (53)). Kapton had the highest $\bar{l}$. It did not neck and exhibited a very diffusive plastic yielding. They claimed from their results that "plastic flow in glassy polymers is of a highly local nature, but tends to become less so as the natural hinge spacing on molecules increases."

In a similar line of reasoning, Haward et al. changed the length of chain stiff segments (persistence length) in a series of polyestercarbonates, and studied its effect on yielding behavior.[56] They made a series of polyestercarbonates from bisphenol A and terephthaloyl/isophthaloyl entities, the structures of which are shown in Figure (54). The phthalate ester can be either terephthalate or isophthalate. By changing the ester block length n or the type of phthalate ester group, the length of chain stiff segment can be changed. For ester block length n of 4, they observed that if the phthalate group was terephthalate, the polyestercarbonate did not exhibit necking or strain softening; whereas, if the phthalate group was isophthalate, the polymer necked and showed post-yield stress drop. The latter had a smaller stiff segment length (persistence length) due to a kink introduced by isophthalate, while the former polymer had a larger stiff segment length. The authors argued that the observed difference was due to differences in strain hardening. In polyestercarbonate with terephthalate groups, the chain was more extended, strain hardening set in earlier than in the polymers with isophthalate groups, where it had a less extended chain configuration.

Further support came from two sets of experimental results. Polyisocyanates were reported to have very large persistence length, and they always exhibit uniform deformation.[56] Based on a stress controlled molecular dynamics simulation of Brown and Clark,[57] McKechnie et al. studied the effect of chain configurations on the stress-strain behavior of glassy polymers.[58] Different configurations of polyethylene-like polymer with different persistence length and trans concentration were prepared by computer, then these polymers were subject to tension. The authors found that polymers with higher persistence length or higher trans content had more

strain hardening. Since these polymers had same chemical structure, the result was less ambiguous, and the effect of chain stiffness on stress-strain behavior was obvious.

Our results do not contradict conjectures of either Argon and Bessonov[55] or Haward et al. .[58] In our polymers, with the incorporation of main chain trans- C-rings, the polymer chains are extended, the persistence length increases, and the polymers are inclined to undergo plastic deformation more diffusively instead of locally. In both Tmc and BPAZ polymers, with the increase in main chain C-ring incorporation, post-yield stress drop decreases; in $Tmc_1C$, TmcCBC, $Z_1C$, and ZCBC, the PYSD is basically 0 (Figure (55)).

Although there is an apparent correlation between chain stiffness and the tendency to diffusive plastic deformation, we believe the strain hardening explanation by Haward et al. [56] is not the only main reason. The arguments pointing to other reasons come from the stress-strain behavior of aged amorphous polymers. PVC quenched from 90°C showed hardly necking or post-yield stress drop, but annealed PVC showed prominent necking and PYSD.[56] This behavior was also observed in amorphous poly(ether ether ketone)[59,60] and in amorphous poly(ethylene terephthalate).[61] In all these polymers, physically aged specimens below Tg exhibited increased yield stress and increased post-yield stress drop compared with those of quenched specimens. There are some reports of the effect of annealing on chain conformational change. Ito et al. proposed that physical aging of amorphous polyethylene terephthalate resulted in a decrease in the amount of trans conformation relative to gauche conformation based on their IR results.[62] However, Garcia reported no change in the relative concentration of trans vs. gauche conformations with annealing of glassy PET in his more recent FTIR measurements.[63] According to Bubeck and Bales,[64] there was no radical change in molecular conformation associated with physical aging. Therefore, from the available data on the effect of annealing on chain conformation, we cannot derive a correlation between PYSD and chain stiffness.

Based on these observations associated with physical aging, we propose that the tendency to uniform plastic deformation is closely related with molecular dynamics. Physical aging results in slowed-down segmental mobility, and longer relaxation times,[65] so the stress localization can not be carried away fast enough to be shared with other segments, therefore, necking takes place, which is accompanied with a drop in stress. Also, physical aging densifies polymers, and reduces the chain spacing. Both the slowed-down chain dynamics and shortened chain spacing lead to increased intermolecular forces, which according to our previous arguments lead to higher resistance to plastic deformation, therefore higher yield stress as observed experimentally. In our polymers, with the increase incorporation of main chain C-rings, the thermal expansion activity is increased, so is the volume fluctuation. When an external stress is imposed, the system tries to comply with it. The more chain dynamics, the faster the stress can be relaxed, and the lesser a chance for stress localization. This is also in accord with what we have found in terms of activation volume. With the increase in main chain C-ring content, the activation volume of yielding also increases, which means more chain segments are involved to relax the imposed external stress. This is obviously much more effective than much localized chain motions.

# 4 Summary

## 4.1 Molecular Motions Probed by DMA

Secondary γ relaxations of three series of polymers have been studied by dynamical mechanical analysis. We have found that the main chain C-rings undergo ring inversion in all the polymers studied. The side chain C-ring in Tmc polymers does not undergo ring inversion, but that of BPAZ does. The relaxation strength of γ relaxation correlates linearly with total C-ring concentration (including side chain C-rings in BPAZ polymers), but not with main chain C-ring content. Main chain and side chain C-rings in BPAZ have the same effect on DMA, indicating main chain C-rings hindered at both ends by polymer segments are activated to at least the same extent as the side chain C-rings where only one end is hindered by polymer segment. But whether the scale of segmental motion increases or not with the incorporation of main chain C-rings cannot be determined without ambiguity from DMA. Because other physical properties, such as CTE, elastic modulus, and yield stress, do not have correlation with the total C-ring concentration, this implies the motion probed by DMA may not be correlated with these properties.

## 4.2 Thermal Expansion Coefficient, Chain Packing, and Elastic Modulus

The thermal expansion coefficient reflects predominantly the expansion of the distance between polymer chains. The increase in LCTE correlates linearly with the main chain C-ring concentration, but not with the total C-ring content. Main chain segmental motion is much more effective in modulating the intermolecular forces than local side chain motions. Chain topology and chain dynamics dictate chain packings. Main chain trans- C-rings can extend polymer chains, which is conducive to good chain packing; the intrachain segmental motion enhanced by main chain C-ring inversion provides the kinetics for the packing process. Thus packing efficiency, as indicated by open hole volume size at low temperature probed by PALS, improves with main chain C-ring content. The relative order of the ranking of CTE values may be different depending on whether hole CTE or bulk CTE is used. Hole CTE can give a more realistic ranking, but bulk CTE sometimes cannot, because it is an "apparent" value.

## 4.3 Glass Transition Temperature and Persistence Length

Main chain motions are enhanced and intermolecular interactions are weakened by the incorporation of main chain C-rings; naturally one would expect a decrease of glass transition temperature. By contrast, Tg increases with main chain C-ring content. This leads us to propose the main factor controlling Tg in our polymers (and possibly for all polymers): chain stiffness, described by persistence length or Kuhn length. Various empirical correlations by many researchers fail to work for polymers with aromatic groups in the main chain. This is mainly because the correlation parameters such as chain steric factor or characteristic ratio reflect only the relative chain stiffening by internal rotation interactions, which do not reflect the inherent segment stiffness of the rotating units.[10] The parameters which can describe chain stiffness on a absolute scale is persistence length or Kuhn length. In terms of persistence length, we have found that as main chain C-ring content increases, persistence length also increases. The main chain C-ring inversion will shorten the length of chain stiff segment slightly by changing C-ring

conformation from equatorial trans to axial trans, so trans C-ring inversion hardly has any negative effect on chain stiffness. On the other hand, if the main chain C-rings have cis configuration, a kink is introduced into polymer chain, which shortens the length of chain stiff segment significantly, therefore a big drop in glass transition temperature is observed. Trans main chain C-rings behave like phenyl groups in stiffening polymer chain segment, but phenyl groups cannot induce large scale segmental motion.

### 4.4 Mechanical Properties

With main chain C-ring incorporation, yield stress/Young's modulus decreases, and the tendency toward uniform plastic deformation increases. The near linear correlation between yield stress and Young's modulus reflects the fact that interchain interaction dominates the deformation behavior.[49,50] But equally important is the intrachain interaction. Intrachain segmental motion enhances volume fluctuation, reduces the effective interacting surface area and time between polymer chains, thus effectively weakening intermolecular interaction. The enhanced segmental motion is reflected not only in the enhanced thermal expansion, reduced yield stress/modulus, but also in the tendency to uniform deformation. Necking is a result of strain localization. If the stress can be relaxed rapidly, it will not result in necking. With increase in main chain C-ring content, segmental motion is enhanced and volume fluctuation increases. With these enhanced dynamics, external stress can be relaxed faster and more effectively, while the tendency to necking and post-yield stress drop is also gradually decreased. The apparent correlation between persistence length and the tendency toward uniform deformation by Haward et al. is systematically observed in our system.

## References


[1] D. Freitag. Prog. Polym. Sci. 19, 1994, 995.

[2] J. Heijboer. Br. Polym. J. 1, 1969, 3.

[3] K. C. Stueben. Journal of Polymer Science: Part A 3, 1965, 3209.

[4] D. Freitag, U. Grigo, P. R. Muller, and W. Nouvertne. In Encyclopedia of Polymer Science, vol. 11. 1988.

[5] R. B. Prime and C. Feger. In Applications of High Temperature Polymers, Ed. R. R. Luise. CRC Press, Inc, 1996.

[6] V. P. Privalko and S. Lipatov. J. Macromol. Sci.-Phys. B9(3), 1974, 551.

[7] R. F. Boyer. Macromolecules 25, 1992, 5326.

[8] X. Lu and B. Z. Jiang. Polymer 32, 1991, 471.

[9] K. K. Chee. Journal of Applied Polymer Scince 43, 1991, 1205.

[10] T. M. Birshtein. Vysokomol. Soyed. A19(1), 1977, 54.

[11] O. Kratky and G. Porod. Recl. Trav. Chim. 68, 1949, 1106.

[12] P. J. Flory. Statistical Mechanics of Chain Molecules. Hanser Publishers, 1989.

[13] Z. D. Xu, N. Hadjichristidis, L. J. Fetters, and J. W. Mays. Advances in polymer science 120, 1995, 1.

[14] C. D. Xiao, J. Y. Jho, and A. F. Yee. Macromolecules 27, 1994, 2761.

[15] L. P. Chen, A. F. Yee, and E. J. Moskala. Macromolecules 18, 1999, 5944.

[16] J. W. Liu and A. F. Yee. Macromolecules 31, 1998, 7865.

[17] J. W. Liu and A. F. Yee. Macromolecules 33, 2000, 1338.

[18] L. P. Chen, A. F. Yee, J. M. Goetz, and J. Schaefer. Macromolecules 31, 1998, 5371.

[19] H. Eyring. J. Chem. Phys. 4, 1936, 283.

[20] R. E. Roberson. J. Chem. Phys. 44, 1966, 3950.

[21] A. S. Argon. Phil. Mag. 28, 1973, 839.

[22] B. Crist. In The Physics of Glassy Polymers, Eds. R. N. Howard and R. J. Young. Chapman & Hall, 1997.

[23] Z. H. Stachurski. Prog. Polym. Sci. 22, 1997, 407.

[24] L. A. Pessan, W. J. Koros, J. C. Schmidhauser, and W. D. Richards. Journal of Polymer Science: Part B: Polymer Physics 33, 1995, 487.

[25] R. Wimberger-Friedl and H. F. M. Schoo. Macromolecules 29, 1996, 8871.

[26] J. Wu. Correlated Motions and Relaxation Behavior in Polycarbonate Copolymers. Ph.D., The University of Michigan, Ann Arbor, Michigan, 1997.

[27] A. F. Yee and S. A. Smith. Macromolecules 14, 1981, 54.

[28] J. S. McHattie, W. J. Koros, and D. R. Paul. Journal of Polymer Scienc: Part B: Polymer Physics 29, 1991, 731.

[29] F. J. Hörth, K. J. Kuhn, J. Mertes, and G. P. Hellmann. Polymer 33(6), 1992, 1223.

[30] M. W. Hellums, W. J. Koros, G. R. Husk, and D. R. Paul. Journal of Membrane Science 46, 1989, 93.

[31] J. Zhao, A. A. Jones, P. T. Inglefield, and J. T. Bendler. Polymer 39(6-7), 1998, 1339.

[32] M. B. Hägg, W. J. Koros, and J. C. Schmidhauser. Journal of Polymer Science: Part B: Polymer Physics 32, 1994, 1625.

[33] J. F. O'Gara, S. G. Desjardins, and A. A. Jones. Macromolecules 14, 1981, 64.

[34] J. Heijboer. Mechanical Properties of Glassy Polymers Containing Saturated Rings. Ph.D., Leiden, Central Lab. Communication 435, 1972.

[35] L. C. E. Struik. In Lecture Notes In Physics, vol. 277. 1987.

[36] F. A. Carey and R. J. Sundberg. Advanced Organic Chemistry, vol. 1. 3 edn. Plenum, 1993.

[37] W. D. Callister, Jr. Materials Science and Engineering An Introduction. 4 edn. John Wiley & Sons, Inc., 1997. Pp 788-790.

[38] P. R. Swan. Journal of Polymer Science 56, 1962, 403.

[39] R. W. Warfield. Die Makromolekulare Chemie 175, 1974, 3285.

[40] Y. Wada, A. Itani, T. Nishi, and S. Nagai. Journal of Polymer Science: Part A-2 7, 1969, 201.

[41] R. E. Barker Jr. Journal of Applied Physics 38(11), 1967, 4234.

[42] M. F. Ashby. Materials Selection in Mechanical Design. 2 edn. Butterworth Heinemann, 1999.

[43] F. Kakali and J. K. Kallitsis. Macromolecules 29, 1996, 4759.

[44] F. Kakali, K. C. Gravalos, and J. K. Kallitsis. Journal of Polymer Science: Part A: Polymer Chemistry 34(8), 1996, 1581.

[45] D. C. Prevorsek and B. T. De Bona. J. Macromol. Sci.-Phys. B19(4), 1981, 605.

[46] D. Freitag and U. Westeppe. Makromol. Chem., Rapid Commun. 12, 1991, 95.

[47] J. W. Liu. The Effect of Enhanced Molecular Mobility on Mechanical Properties. Ph.D., The University of Michgian, 1999.

[48] R. J. Young and P. A. Lovell. Introduction to Polymers. 2 edn. Chapman & Hall, 1996.

[49] L. Yang. Molecular Dynamics Simulation of the Glass Transition and Deformation Behavior of Amorphous Polymers. Ph.D., The University of Michigan, Ann Arbor, Michigan, 1997.

[50] C. F. Fan. Macromolecules 28, 1995, 5215.

[51] N. Brown. Materials Science and Engineering 8, 1971, 69.

[52] L. C. E. Struik. Journal of Non-Crystalline Solids 131-133, 1991, 395.

[53] M. Song, D. J. Hourston, and H. M. Pollock. Journal of Applied Polymer Science 59, 1996, 173.

[54] N. Brown and I. M. Ward. Journal of Polymer Science A2 6, 1968, 607.

[55] A. S. Argon and M. I. Bessonov. Philosophical Magazine 35(4), 1977, 917.

[56] R. N. Haward et al. Colloid and Polymer Science 258(6), 1980, 643.

[57] D. Brown and J. H. R. Clarke. Macromolecules 24(8), 1991, 2075.

[58] J. I. McKechnie, R. N. Haward, D. Brown, and J. H. R. Clarke. Macromolecules 26, 1993, 198.

[59] D. J. Kemmish and J. N. Hay. Polymer 26, 1985, 905.

[60] V. Capodanno, E. Petrillo, G. Romano, R. Russo, and V. Vittoria. Journal of Applied Polymer Science 65, 1997, 2635.

[61] A. Aref-Azar, F. Biddlestone, J. N. Hay, and R. N. Haward. Polymer 24, 1983, 1245.

[62] E. Ito, K. Yamamoto, Y. Kobayashi, and T. Hatakeyama. Polymer 19(1), 1978, 39.

[63] D. Garcia. In Proceedings of the 12th North American Thermal Analysis Society

Conference. 1983.

[64] R. A. Bubeck and S. E. Bales. Polymer Engineering and Science 24(10), 1984, 1142.

[65] L. C. E. Struik. Physical Aging in Amorphous Polymers and Other Materials. Elsevier, 1978.

[66] Molecular Simulations Inc., 9685 Scranton Road, San Diego, CA 92121-3752.

[67] S. L. Mayo, B. D. Olafson, and W. A. Goddard. J. Phys. Chem. 94, 1990, 8897.

[68] The conformations and configurations were generated and energetically minimized using Cerius2 molecular modeling software (version 3.5) from Molecular Simulations Inc,[68] with the atom force potentials being described by the DREIDING II force field.[69]

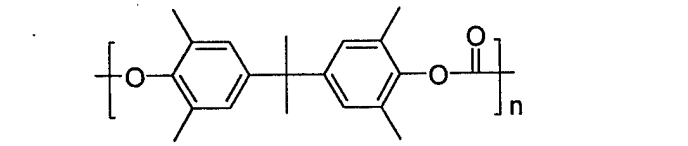

polycarbonate of tetramethyl bisphenol A

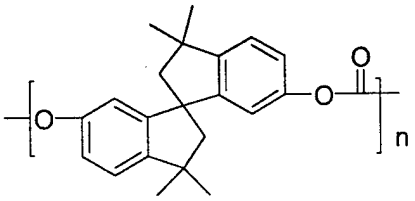

polycarbonate of SBI

Figure 1: Structures of polycarbonates of SBI and tetramethyl bisphenol A

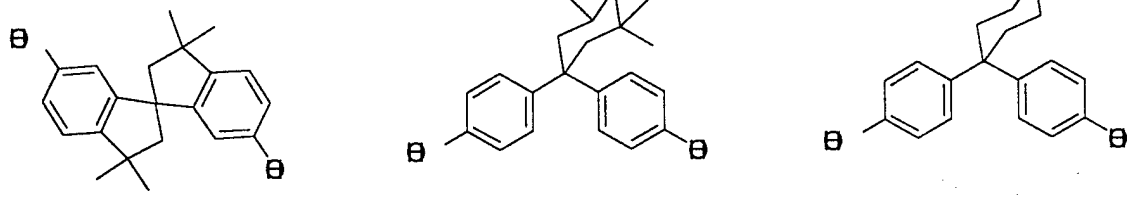

B Tmc BPAZ

Figure 2: The chemical structures of bisphenol monomers: SBI, Tmc and BPAZ

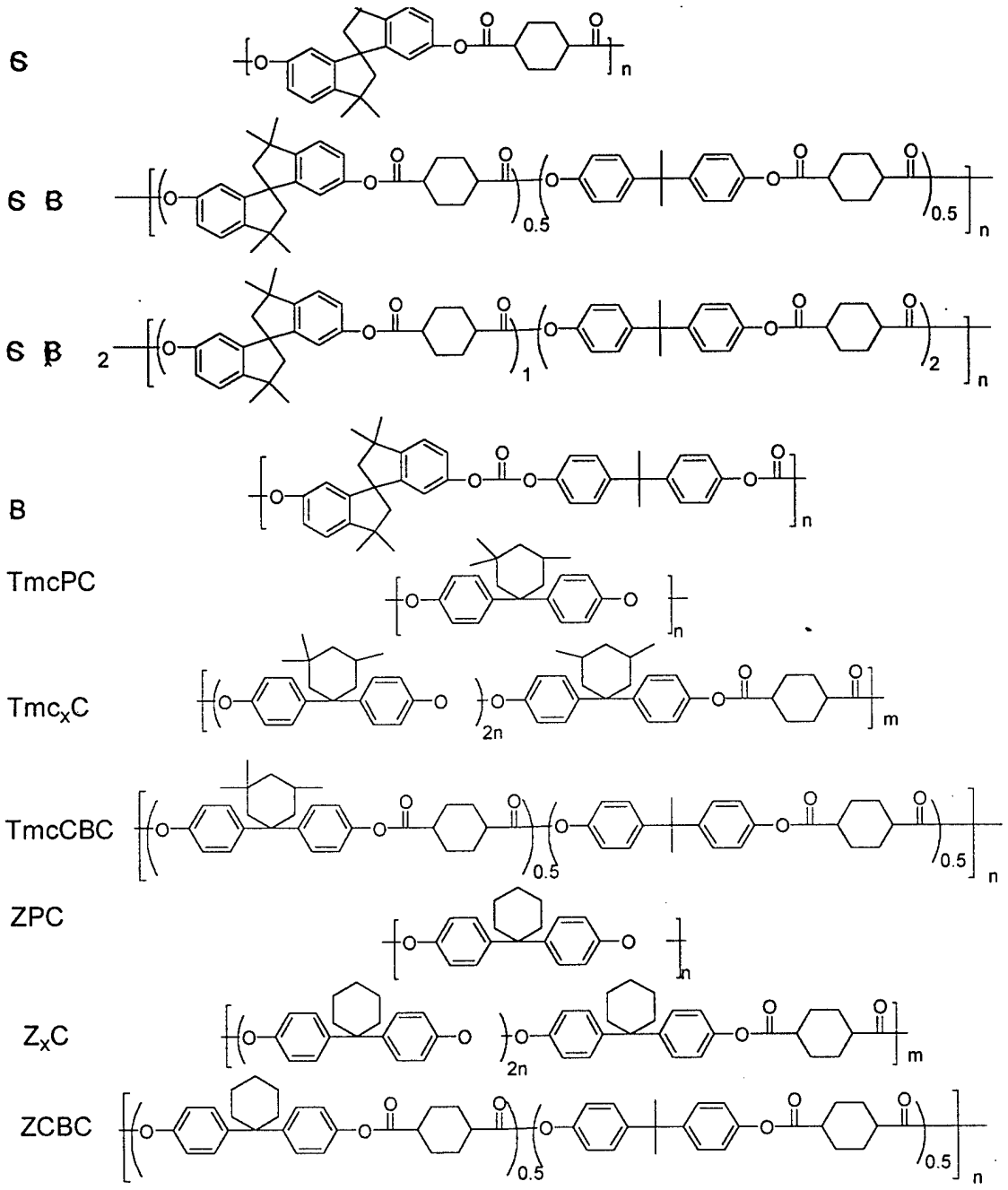


Figure 3: Chemical structures and short names for all the polycarbonates, polyesters and polyestercarbonates.

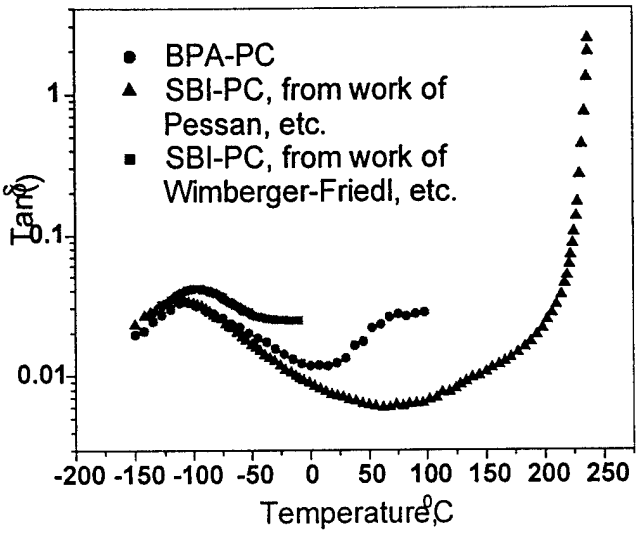


Figure 4: DMA spectra of BPA-PC, SBI-PC, SB at 1 Hz

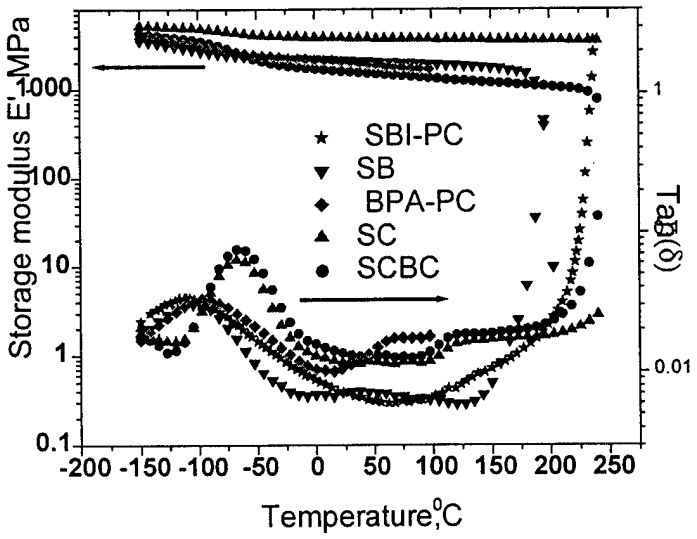


Figure 5: DMA spectra of SBI-PC, SB, SC, BPA-PC and SCBC at 1Hz.

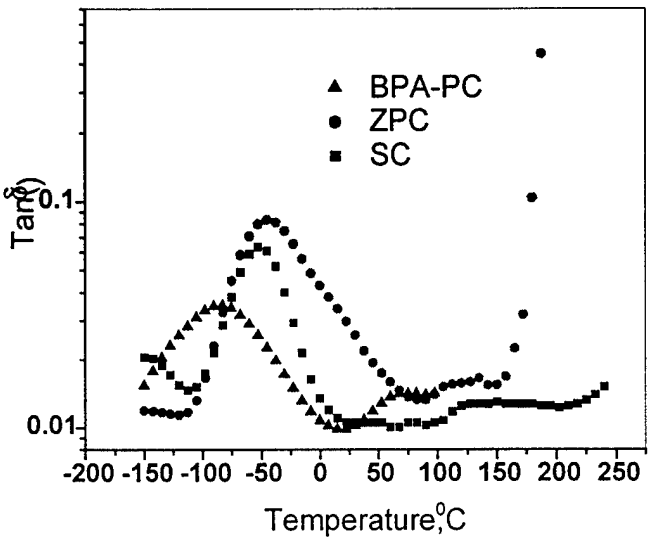


Figure 6: DMA spectra of ZPC and BPA-PC at 10 Hz.

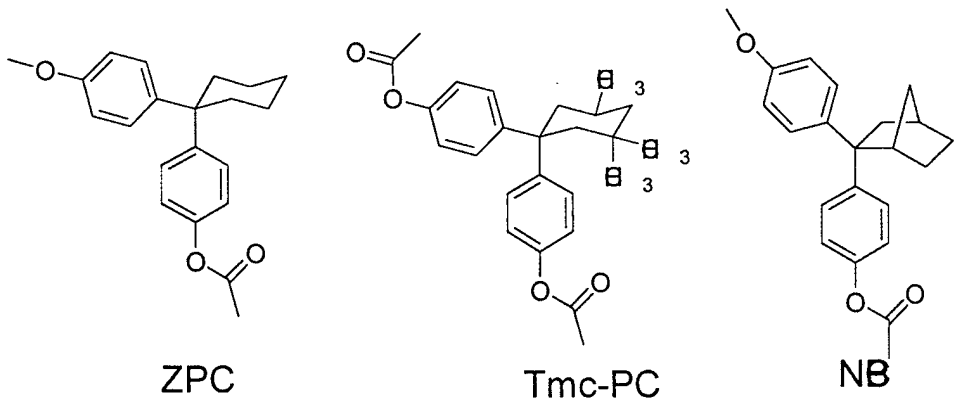


Figure 7: Chemical structures of ZPC, TmcPC and NBPC.

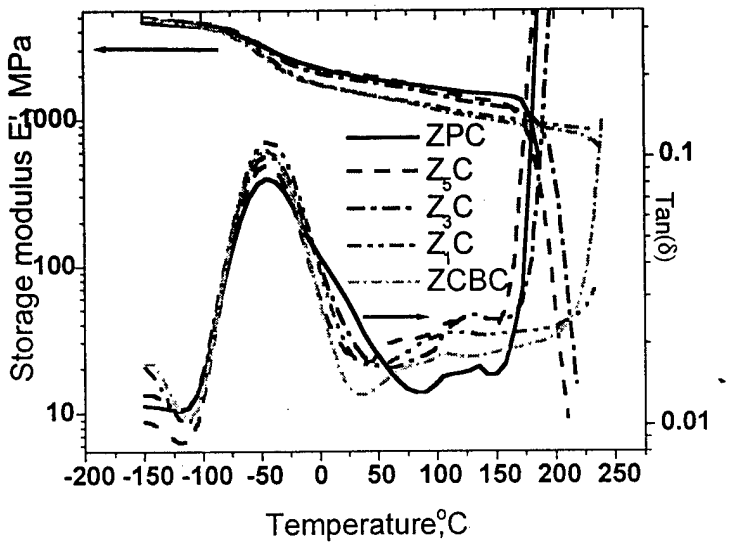


Figure 8: The DMA spectra of ZPC, $Z_xC$ and ZCBC at 10 Hz.

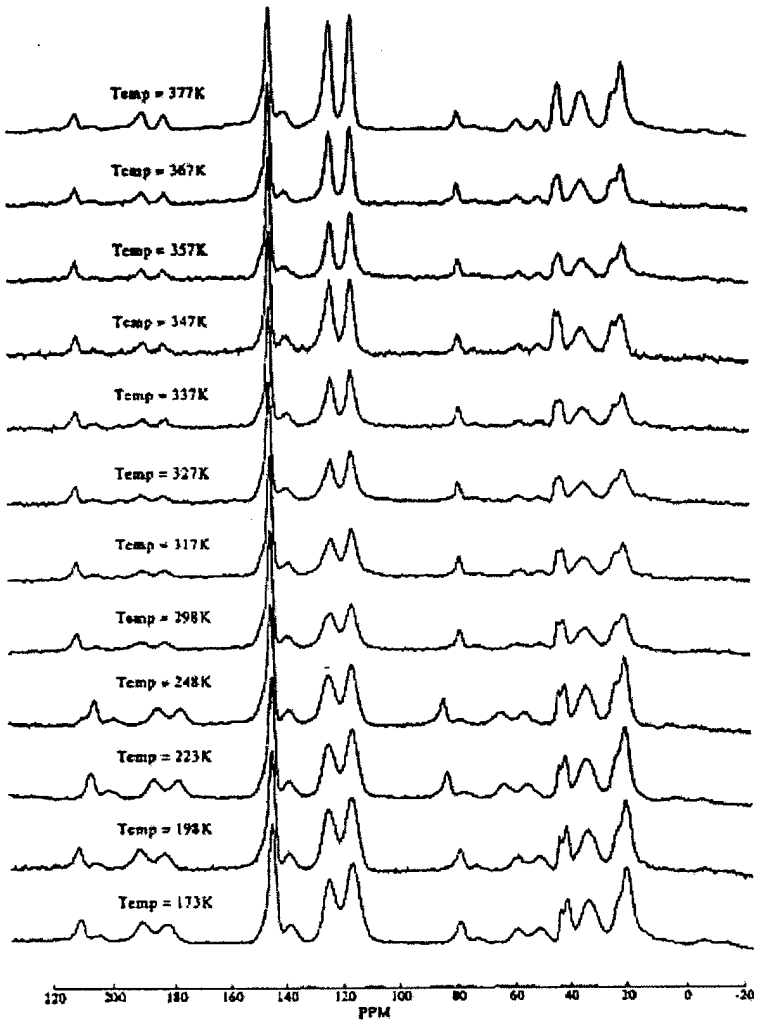


Figure 9: $^{13}$C-NMR variable temperature, solid state spectra of ZPC using CPMAS.[31]

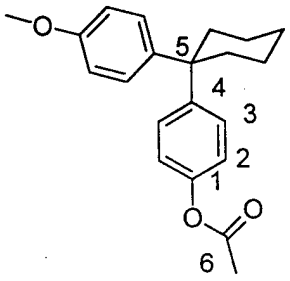


Figure 10: Labeling in ZPC.

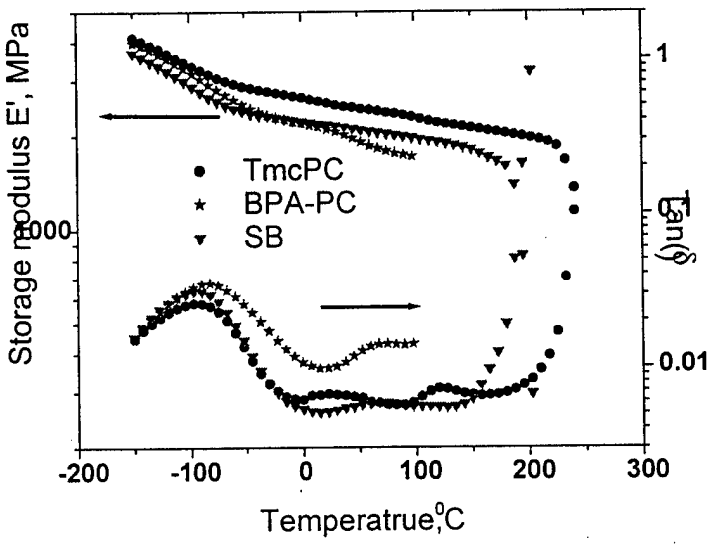


Figure 11: γ relaxation of TmcPC, SB and BPAPC at 10 Hz.

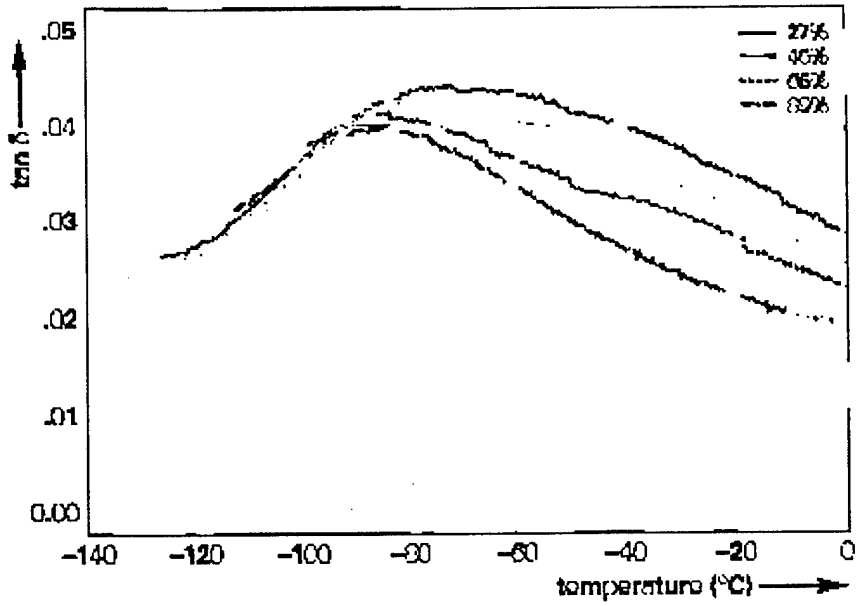


Figure 12: Mechanical loss spectra of copolymers of SBI and BPA with the compositions as indicated in vol% SBI.[25]

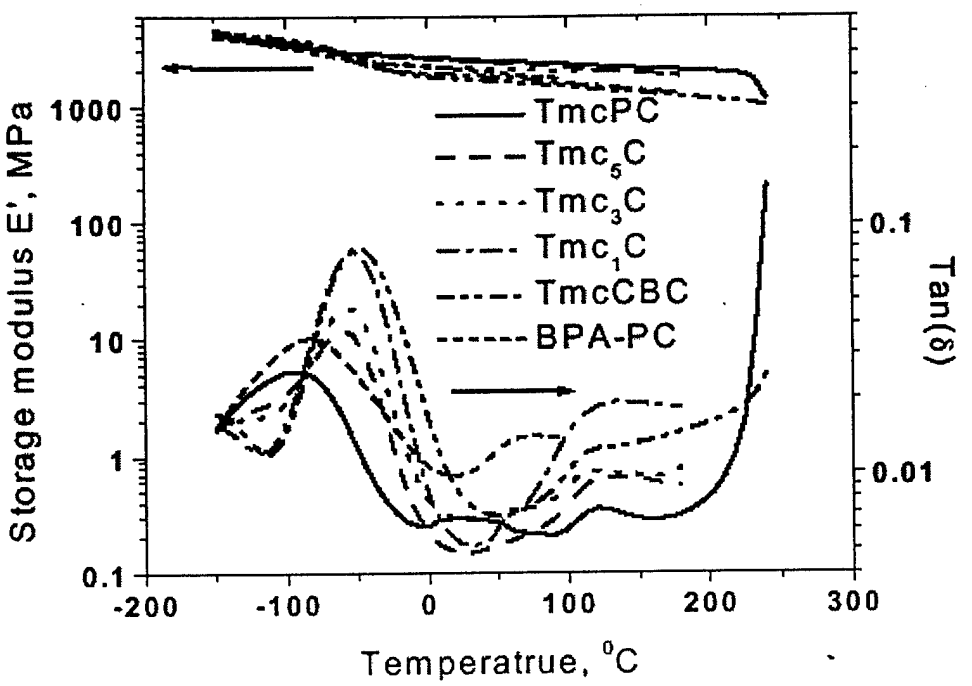


Figure 13: The γ relaxation of polymers based on Tmc at 10 Hz.

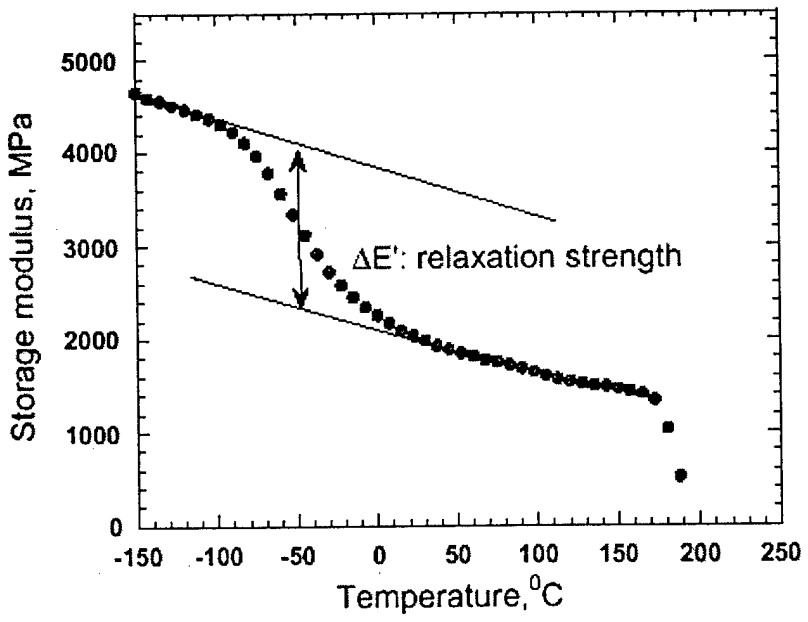


Figure 14: Determination of relaxation strength $\Delta E'$ from a E' vs T curve.

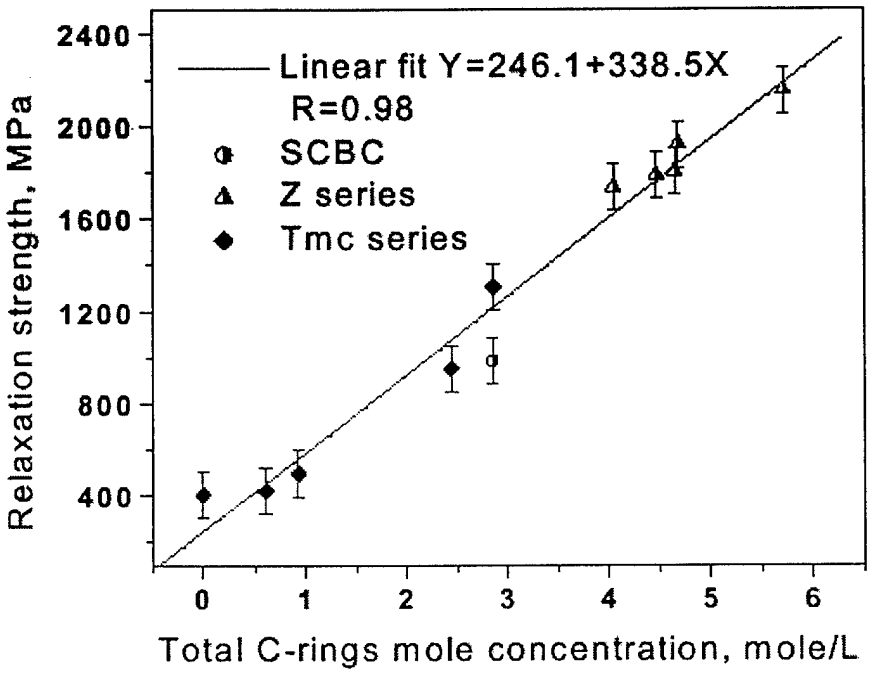


Figure 15: The correlation between the relaxation strength and the total C-rings mole concentration for polymers based on SBI, Tmc and BPAZ.

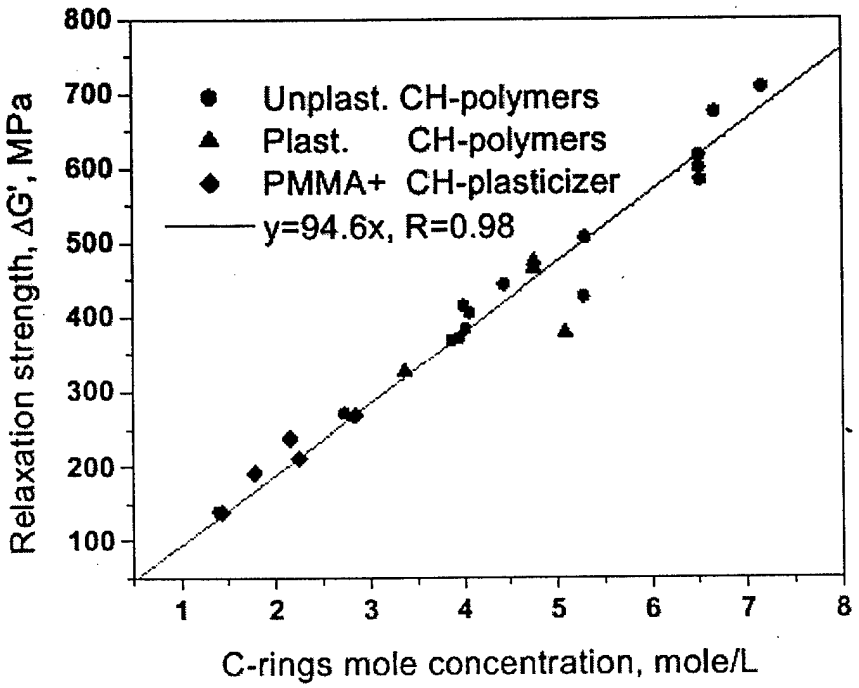


Figure 16: Relaxation strength of cyclohexyl motion vs. C-ring concentration for polymers containing the cyclohexyloxycarbonyl group in the polymer or in the plasticizer.

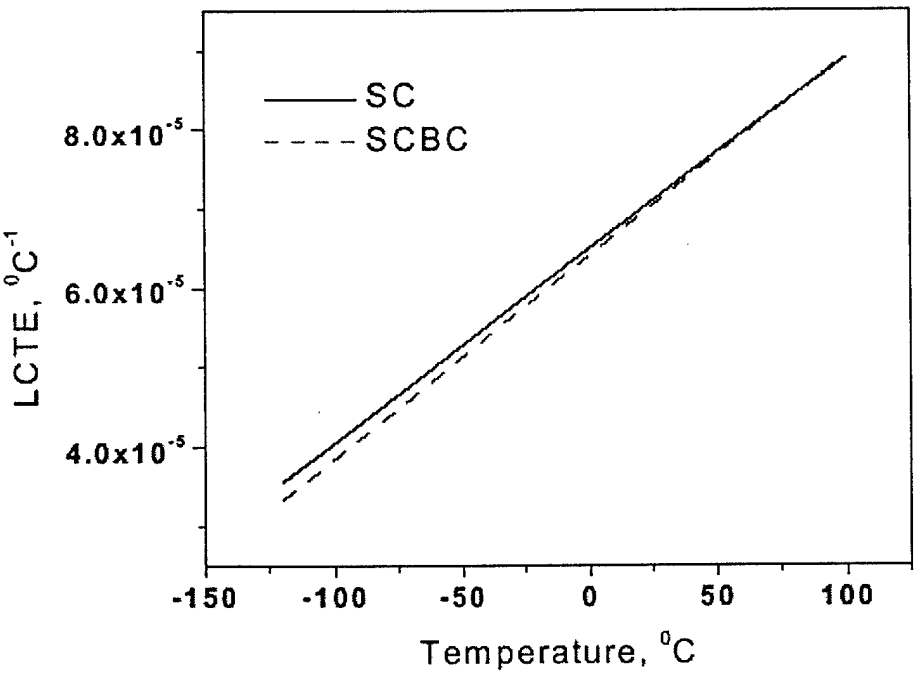


Figure 17: The LCTE change with temperature for SC and SCBC.

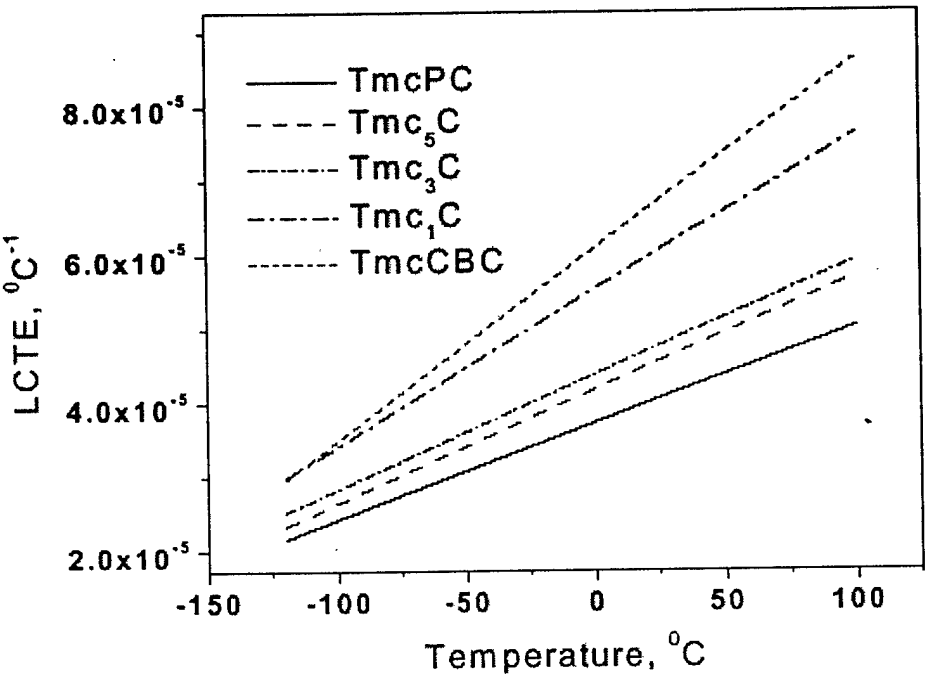


Figure 18: The LCTE change with temperature for polymers of Tmc series.

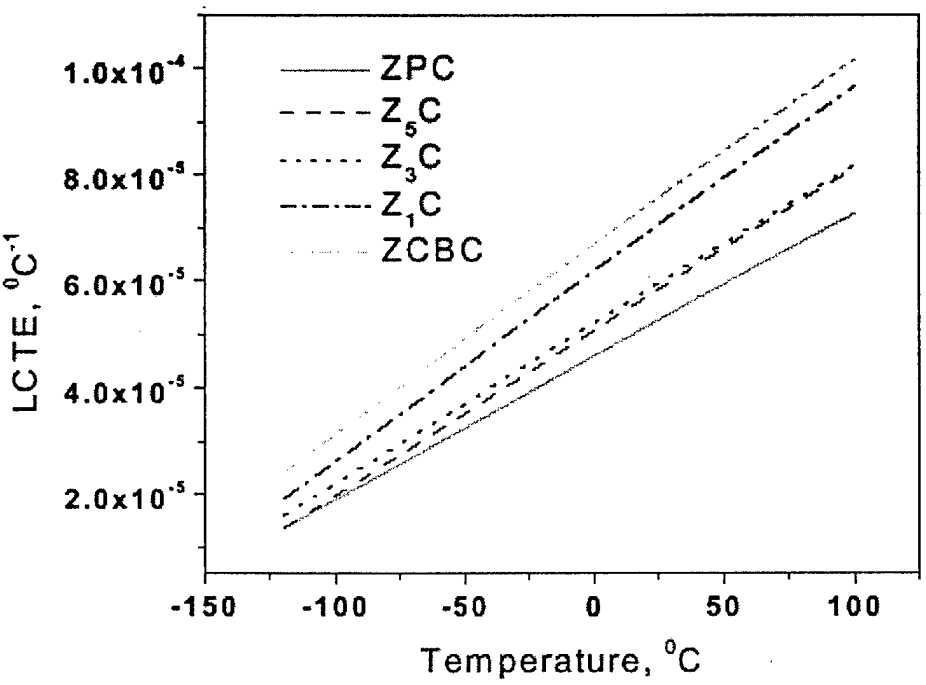


Figure 19: The LCTE change with temperature for polymers of BPAZ series.

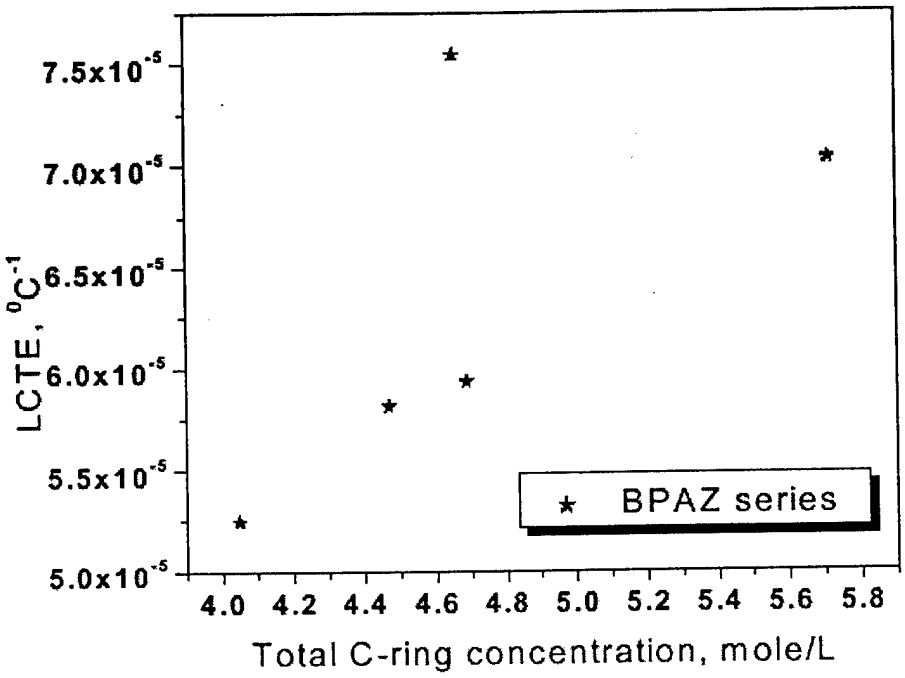


Figure 20: LCTE change with total C-ring concentration at room temperature for BPAZ polymers.

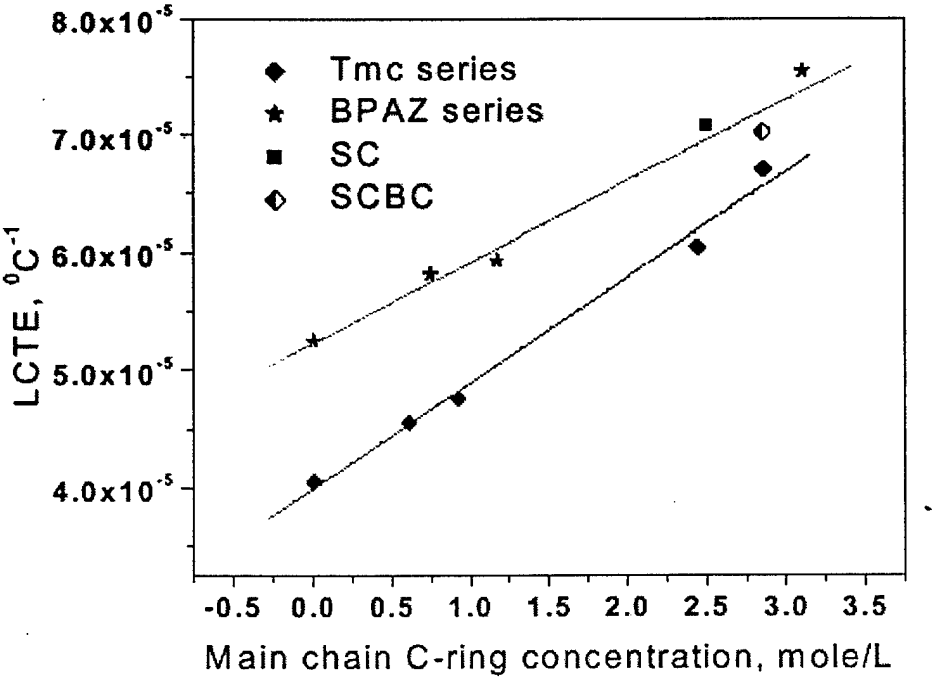


Figure 21: LCTE change with main chain C-ring concentration at room temperature for SBI, Tmc and BPAZ polymers.

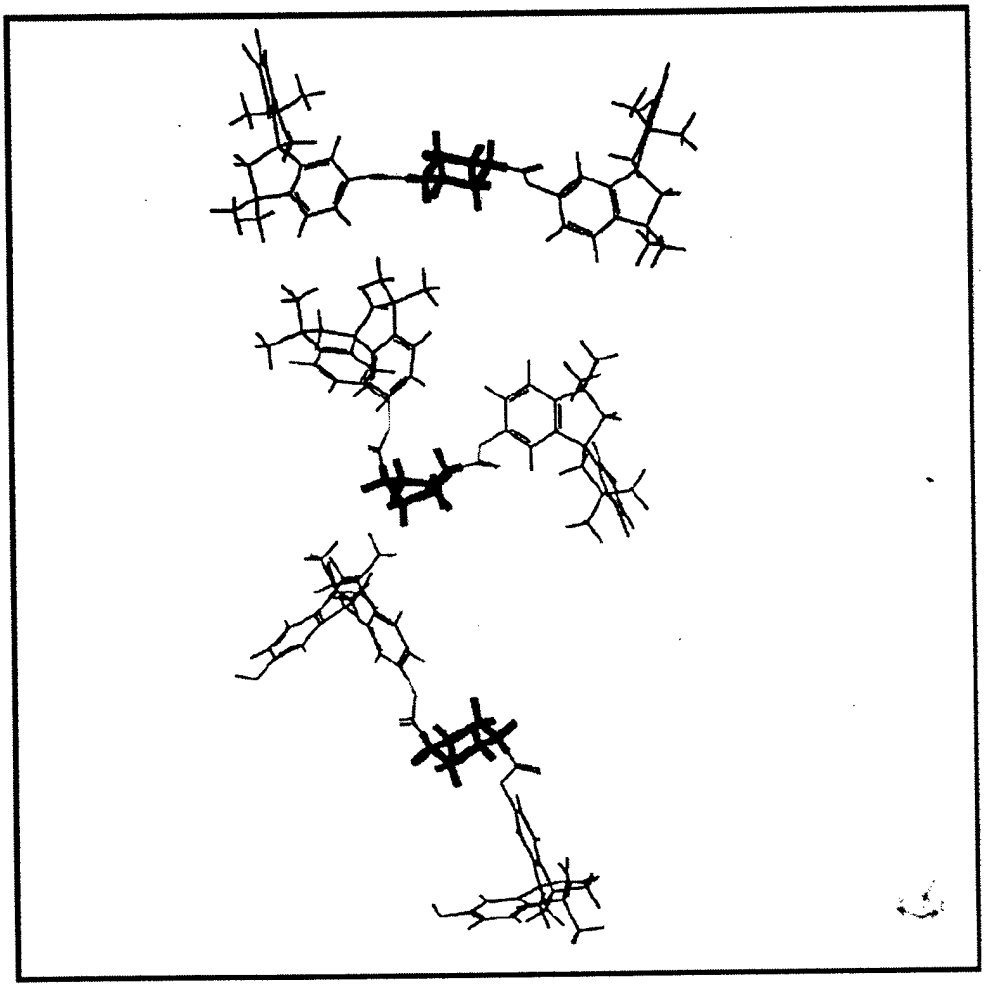

Figure 22: Illustration of chair-boat-chair conformational transition of a main chain C-ring, bulky and rigid SBI entities are linked as neighbors.

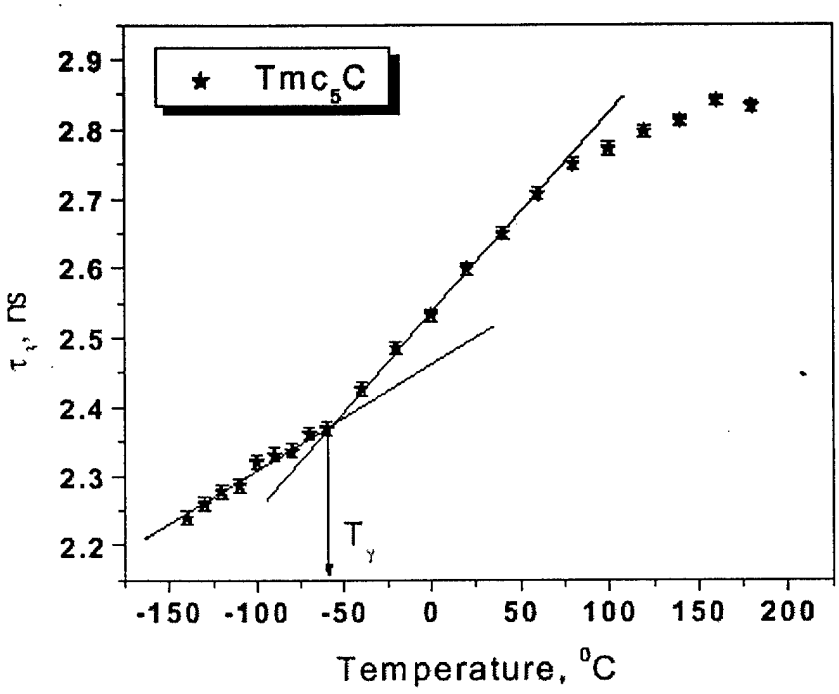


Figure 23: Detection of γ relaxation from PALS curve for $Tmc_5C$.

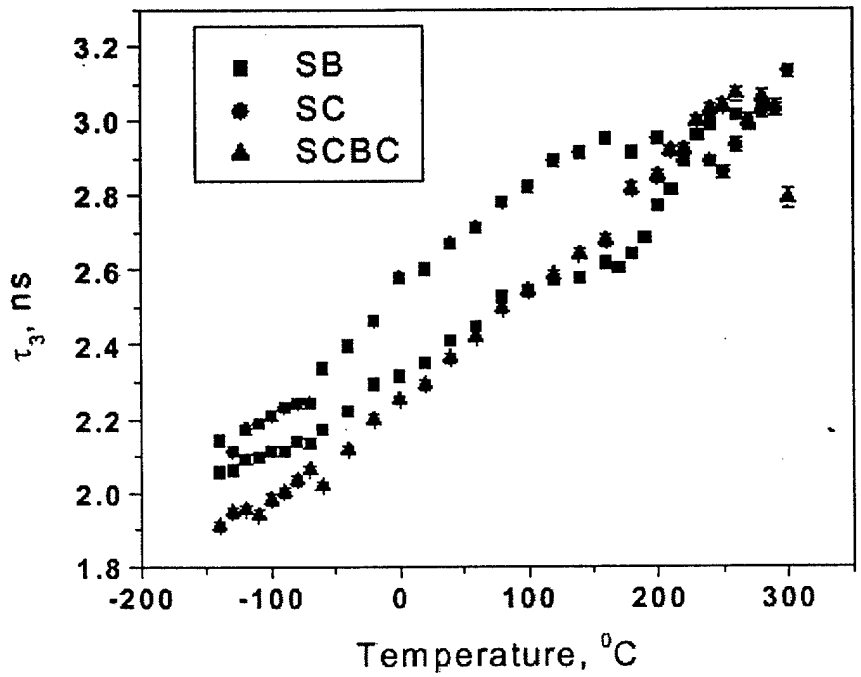


Figure 24: change in the lifetime of o-Ps ( $\tau_3$) with temperature for SBI polymers.

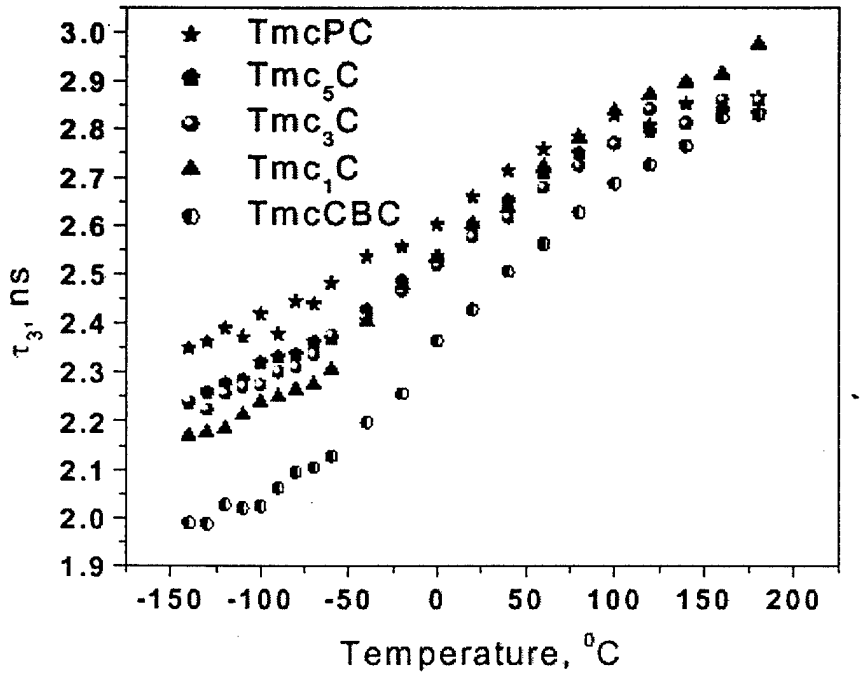


Figure 25: change in the lifetime of o-Ps ( $\tau_3$) with temperature for Tmc polymers.

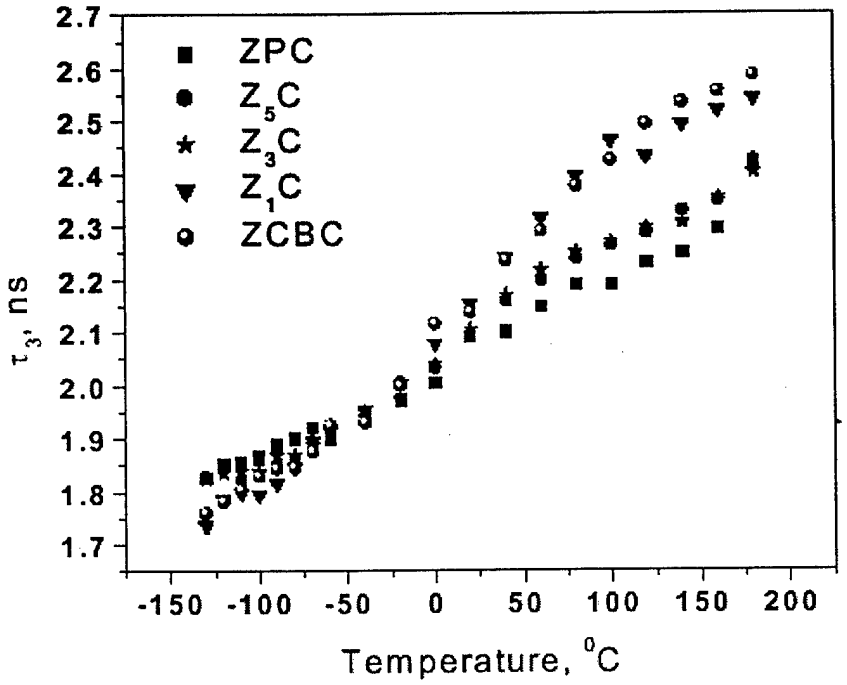


Figure 26: change in the lifetime of o-Ps ( $\tau_3$ ) with temperature for BPAZ polymers.

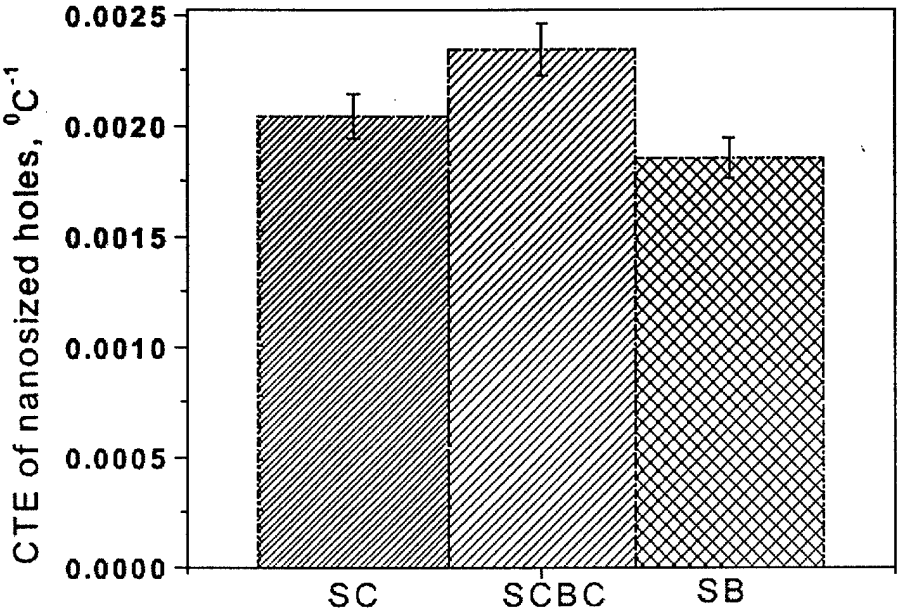


Figure 27: CTE of nanosized holes of SC, SCBC and SB at 24°C

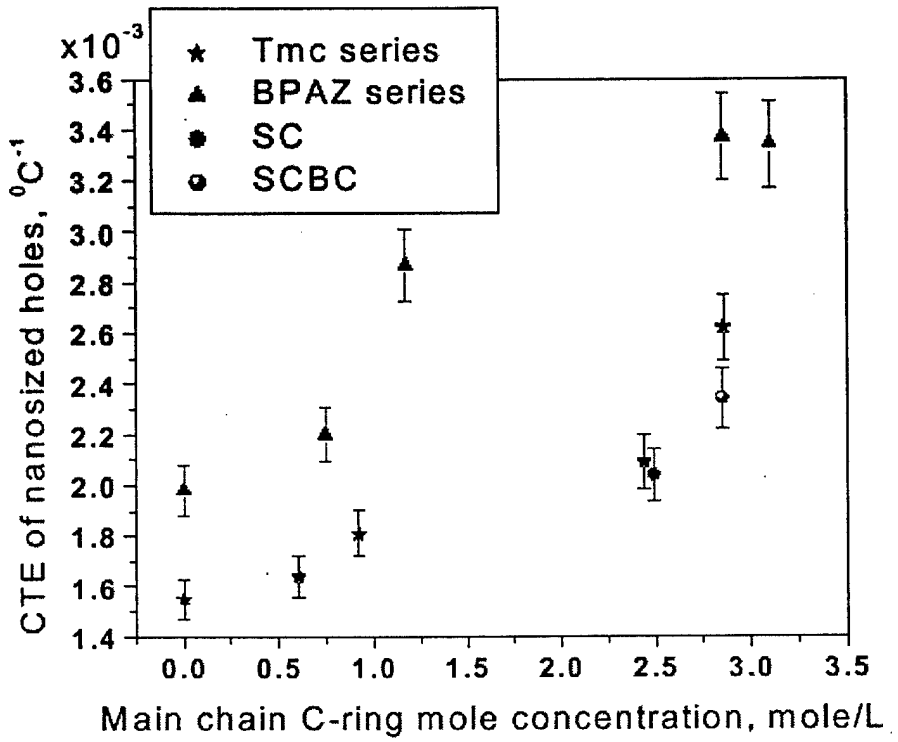


Figure 28: CTE of nanosized holes of all the polymers at 24°C.

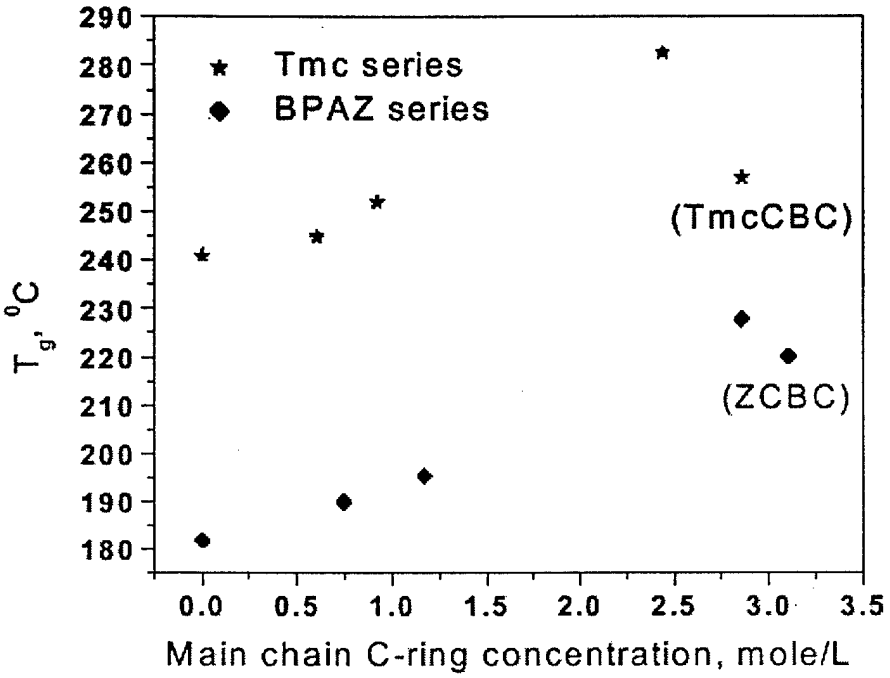


Figure 29: Glass transition temperature change with main chain C-ring incorporation.

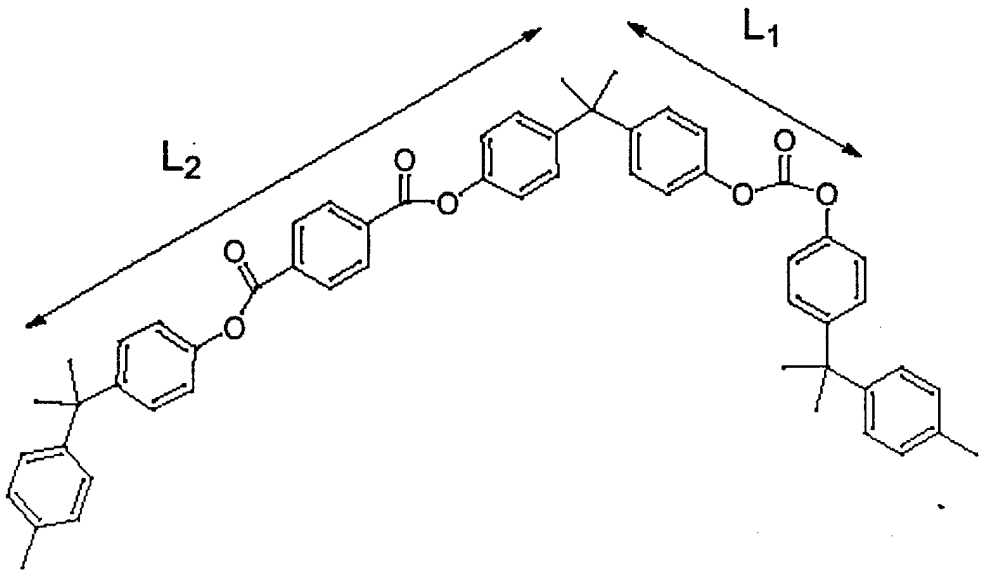


Figure 30: Part of a polyestercarbonate chain: notice the change in stiff segment length introduced by terephthalate group.[45]

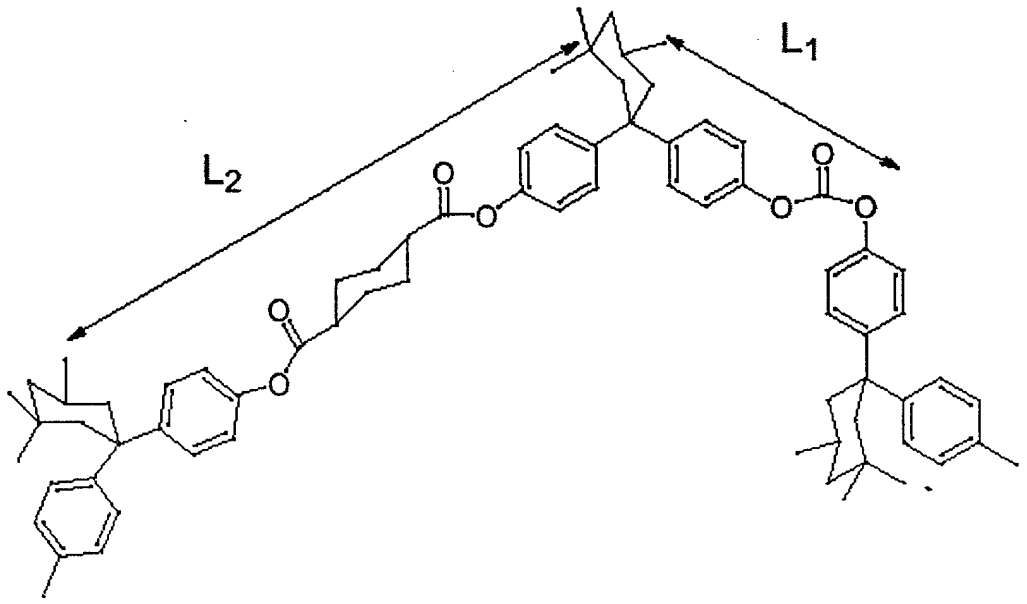


Figure 31: Part of a polyestercarbonate chain of Tmc: notice the increased stiff segment length introduced by trans main chain C-rings.

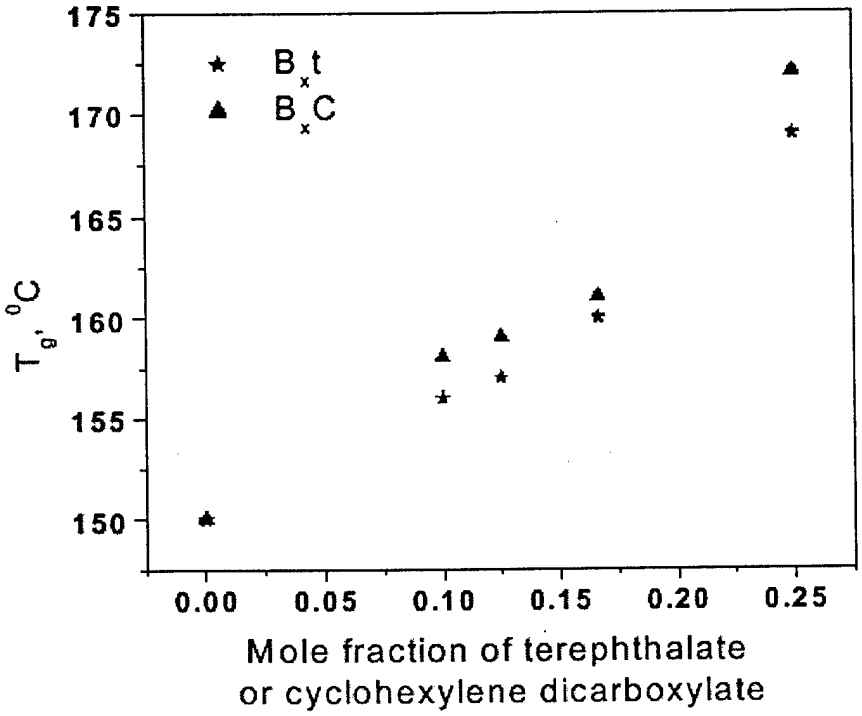


Figure 32: Tg's of $B_x$t and $B_x$C, x is the block length of polycarbonate.[26,47]

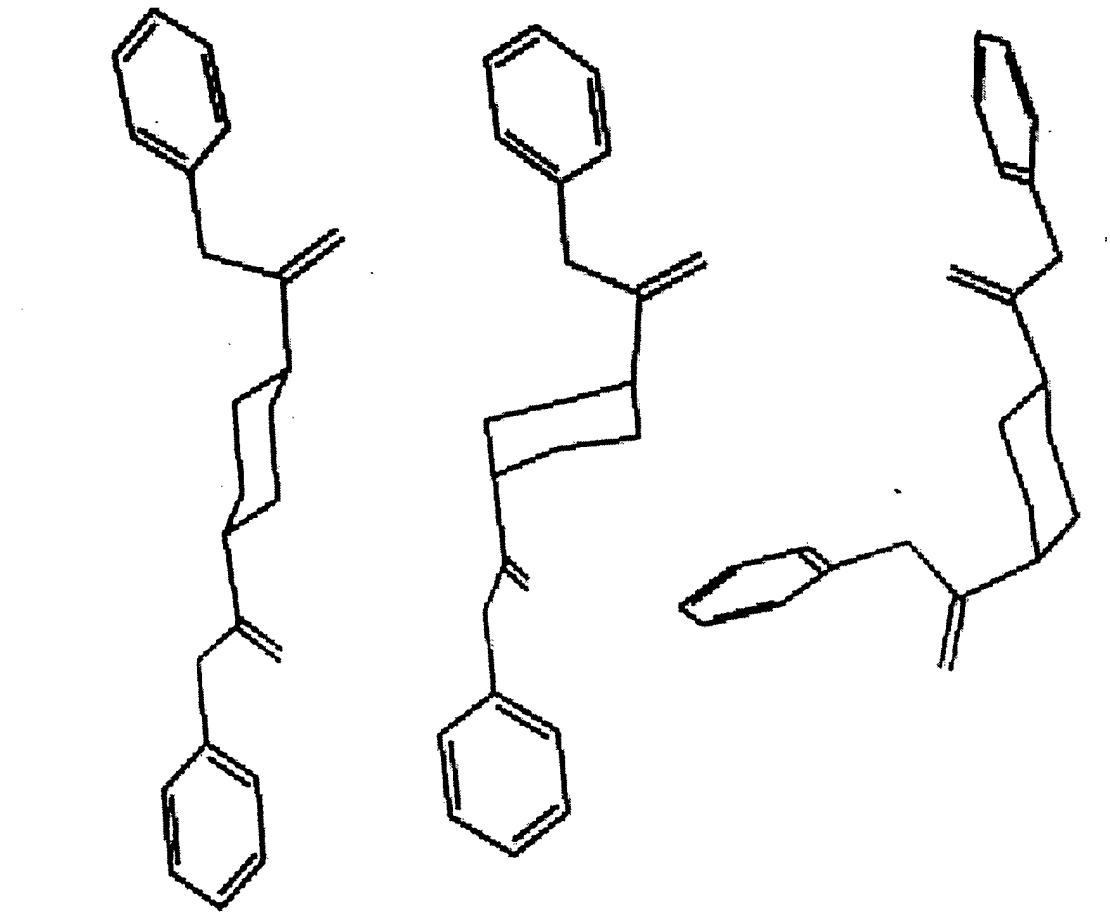


Figure 33: Different configurations and conformations and their effect on the length of stiff segment.[68]

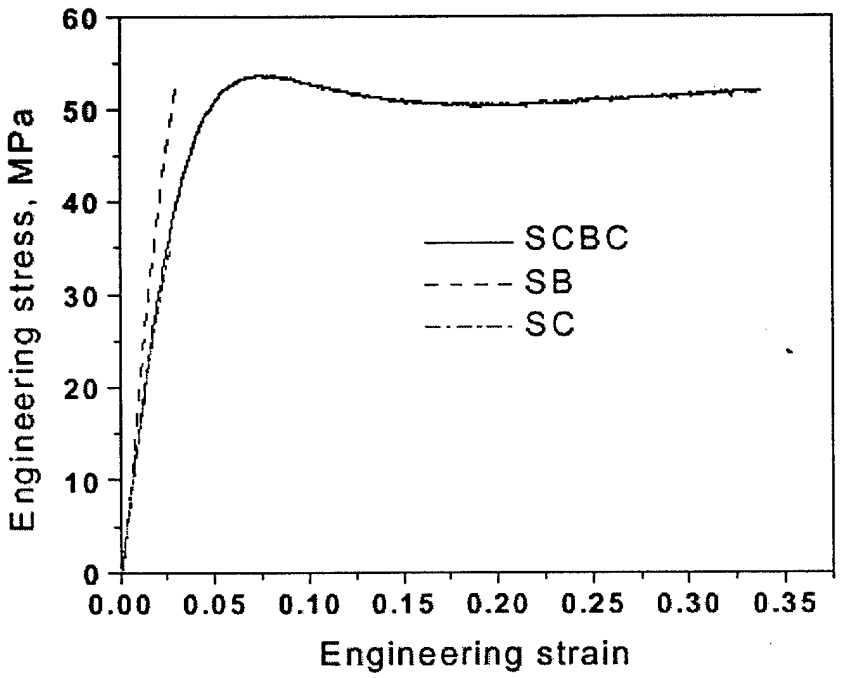


Figure 34: Tensile behavior of SCBC, SB and SC at a strain rate of $2.1\_10^{-2}$ $s^{-1}$, T=24°C.

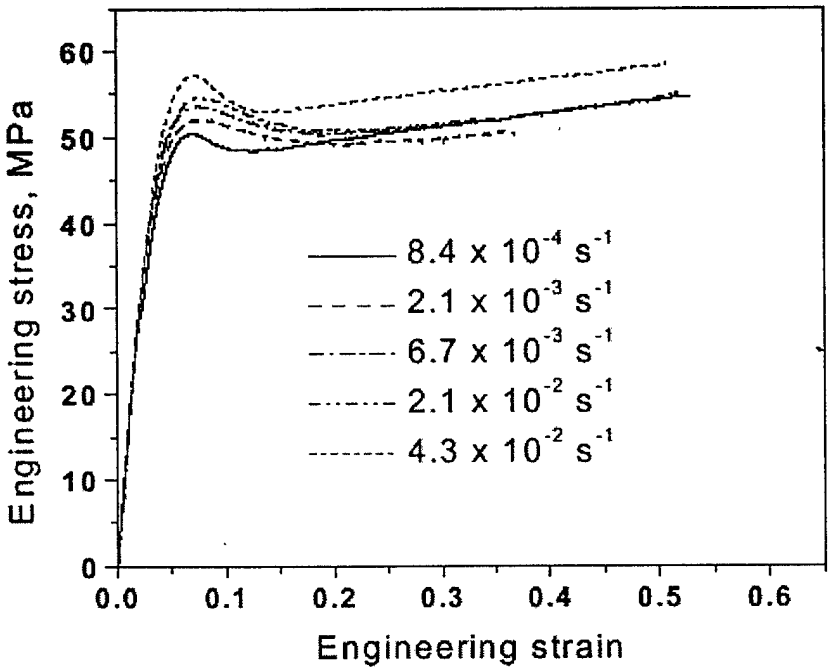


Figure 35: Tensile behavior of SCBC at different strain rate, T=24°C.

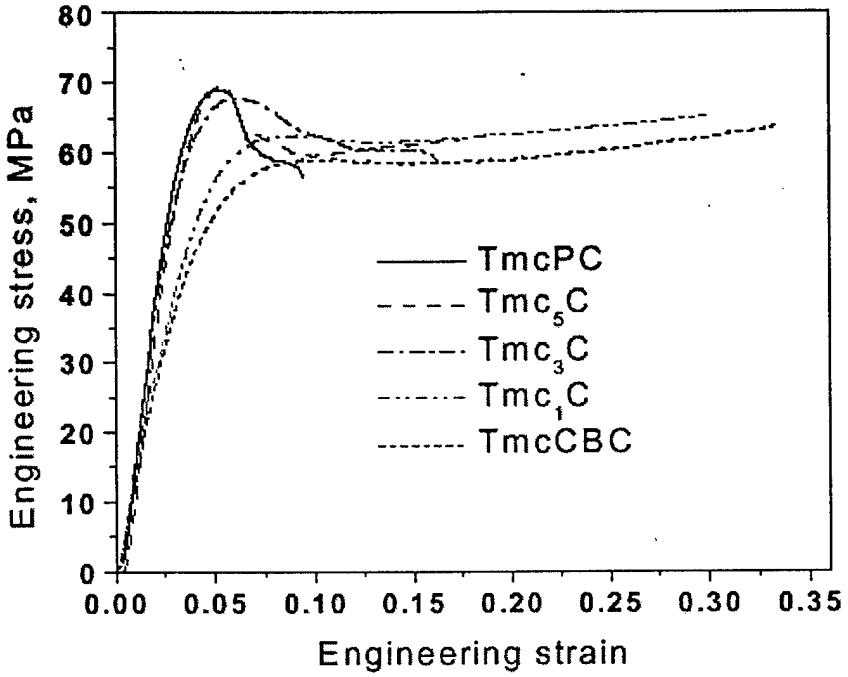


Figure 36: Tensile behavior of Tmc polymers at a strain rate of $2.1\_10^{-2}$ $s^{-1}$, T=24°C.

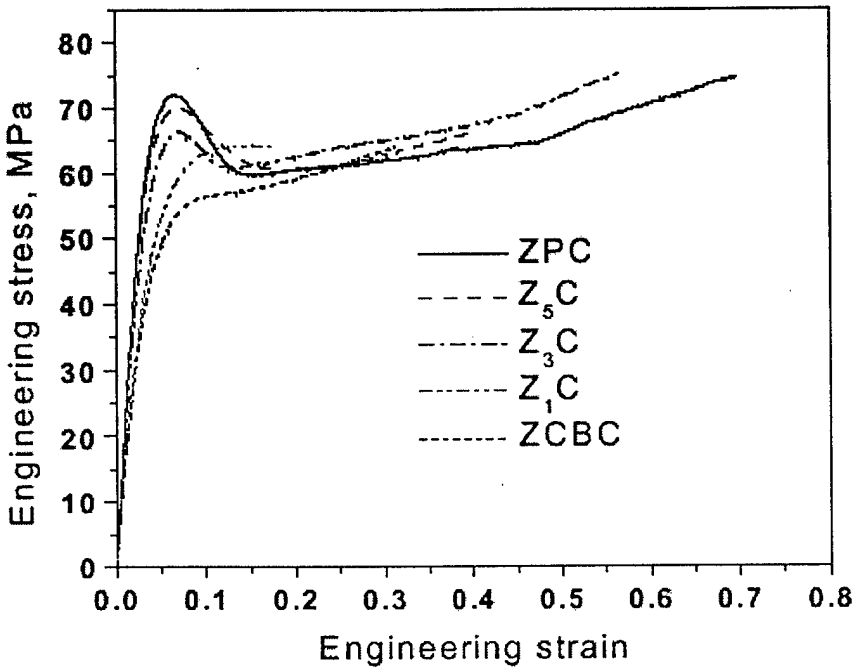


Figure 37: Tensile behavior of BPAZ polymers at a strain rate of $2.1\_10^{-2}$ $s^{-1}$, T=24°C.

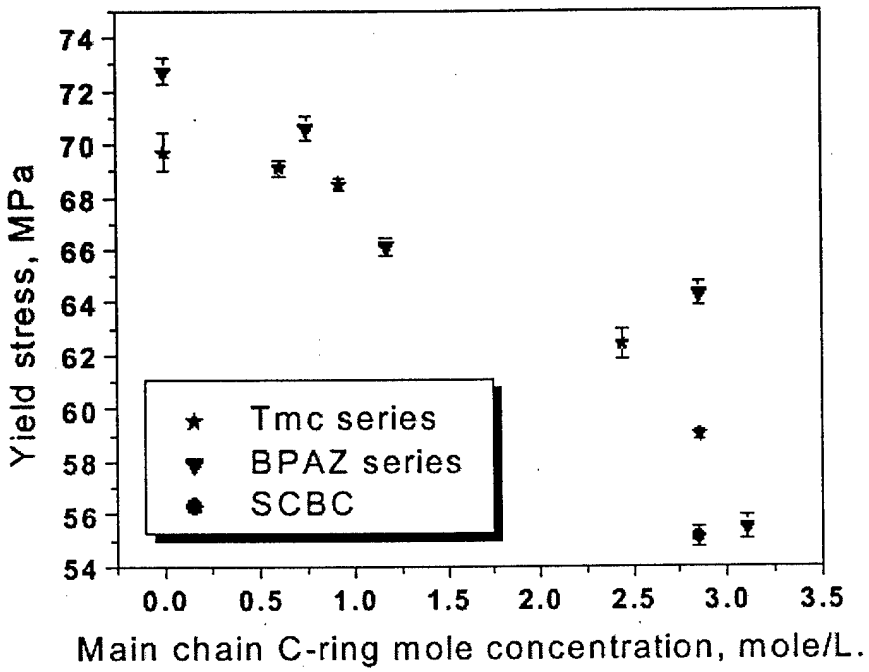


Figure 38: The change in yield stress with the change in main chain C-ring concentration, T=24°C.

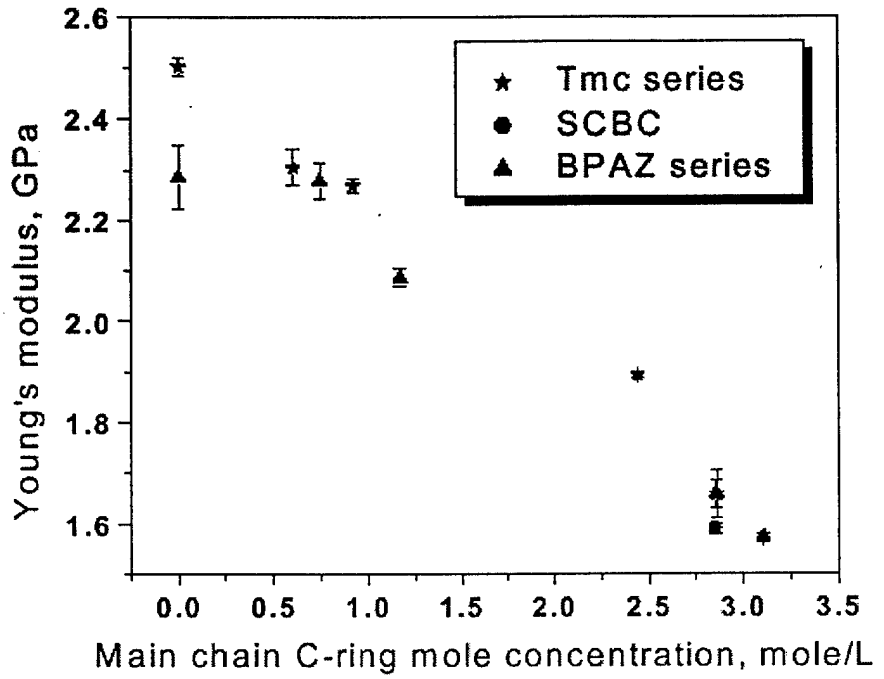


Figure 39: The change in Young's modulus with the change in main chain C-ring concentration at a strain rate of $2.1\_10^{-2}$ $s^{-1}$.

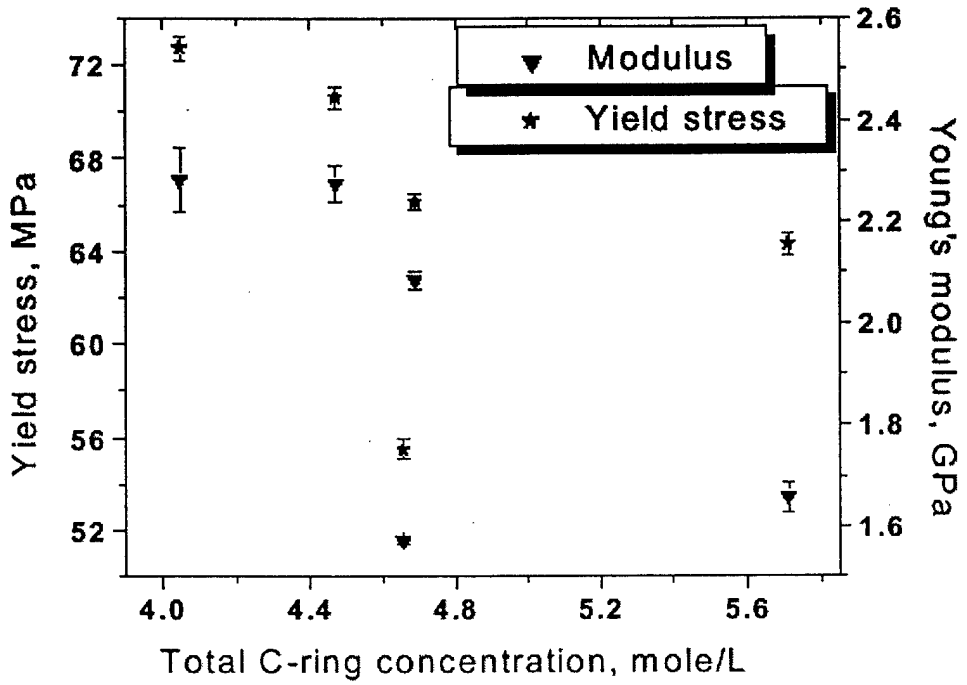


Figure 40: The change in yield stress/Young's modulus with the change in total C-ring concentration for BPAZ polymers at a strain rate of $2.1\_10^{-2}$ $s^{-1}$.

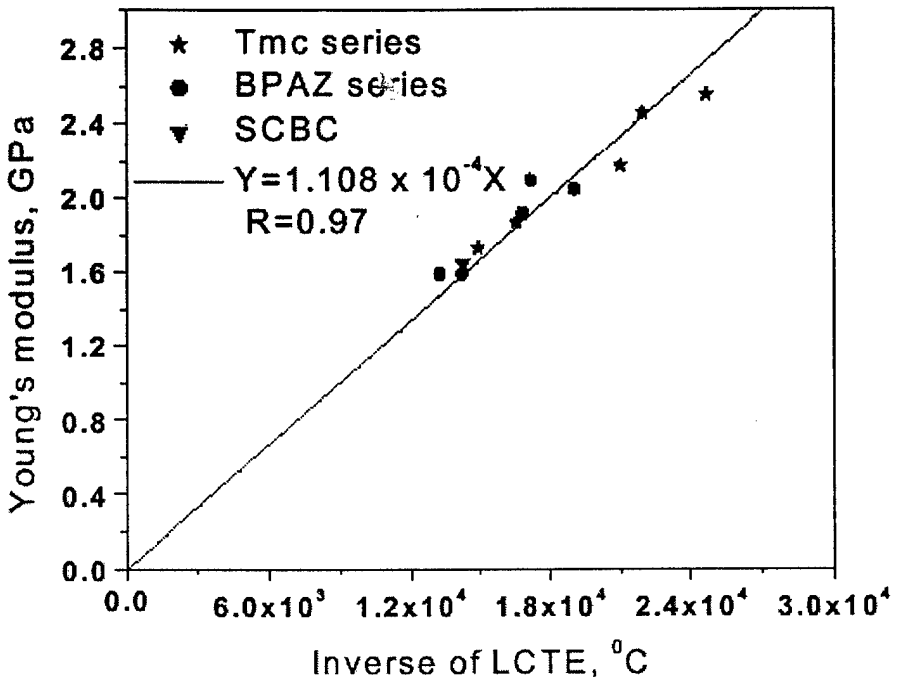


Figure 41: Correlation between Young's modulus and the inverse of LCTE, strain rate is $2.1\_10^{-2}\ s^{-1}$.

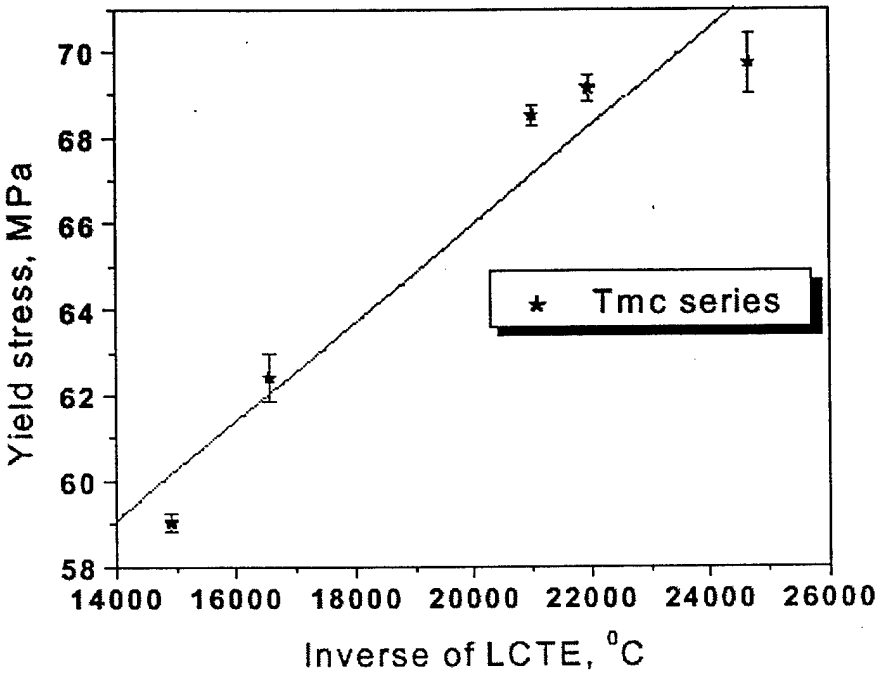


Figure 42: Correlation between yield stress and the inverse of LCTE for Tmc polymers, strain rate is $2.1\_10^{-2}$ $s^{-1}$.

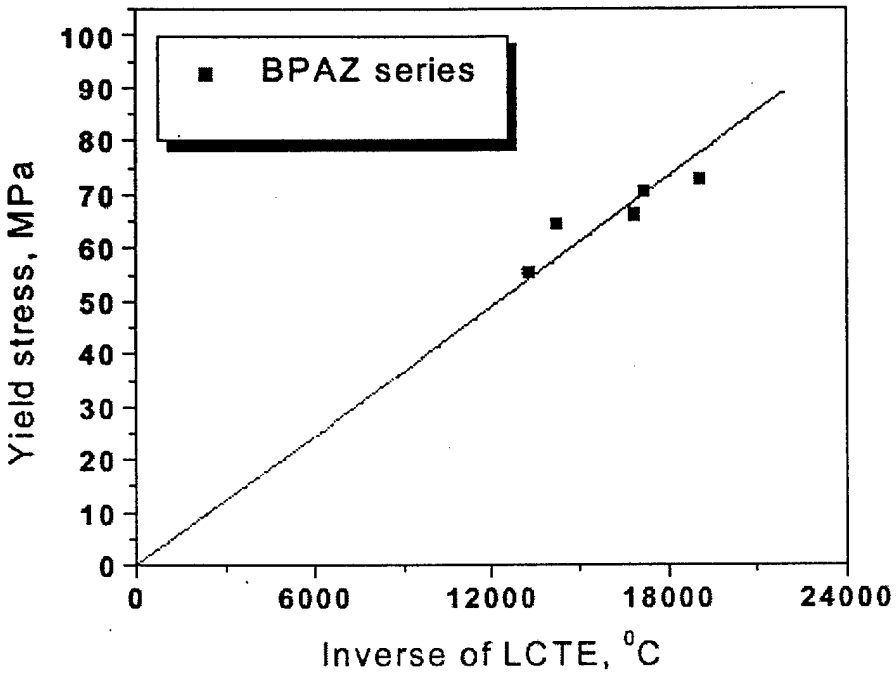


Figure 43: Correlation between yield stress and the inverse of LCTE for BPAZ polymers, stain rate is $2.1\_10^{-2}$ $s^{-1}$.

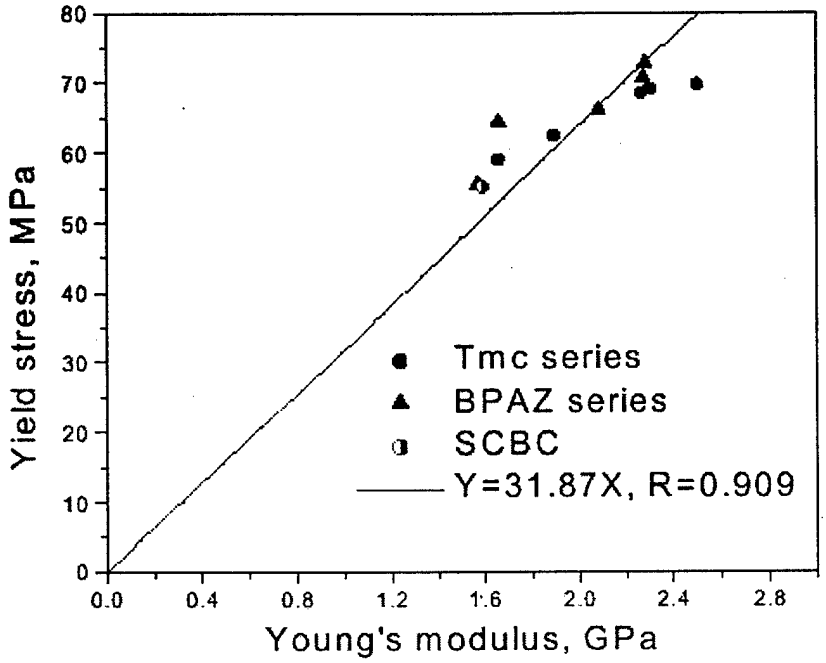


Figure 44: Correlation between Young's modulus and yield stress at a strain rate of $2.1\_10^{-2}$ $s^{-1}$.

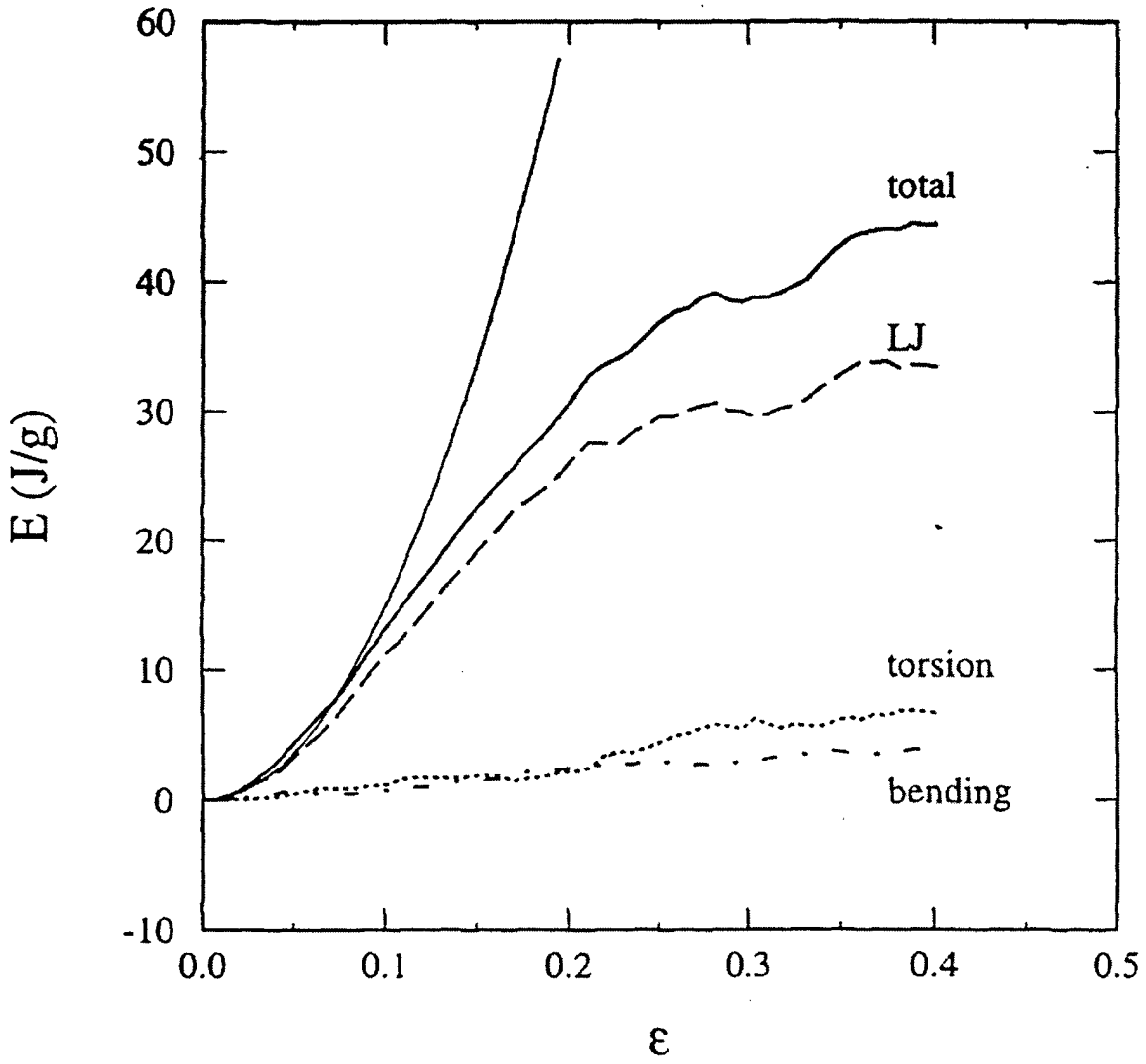


Figure 45: The average bending, torsional, non-bonded Lennard-Jones, and total internal energies versus strain during tensile tests at 100K. The thin solid line indicates how the energy of the system would evolve with strain if the deformation was purely elastic.[49]

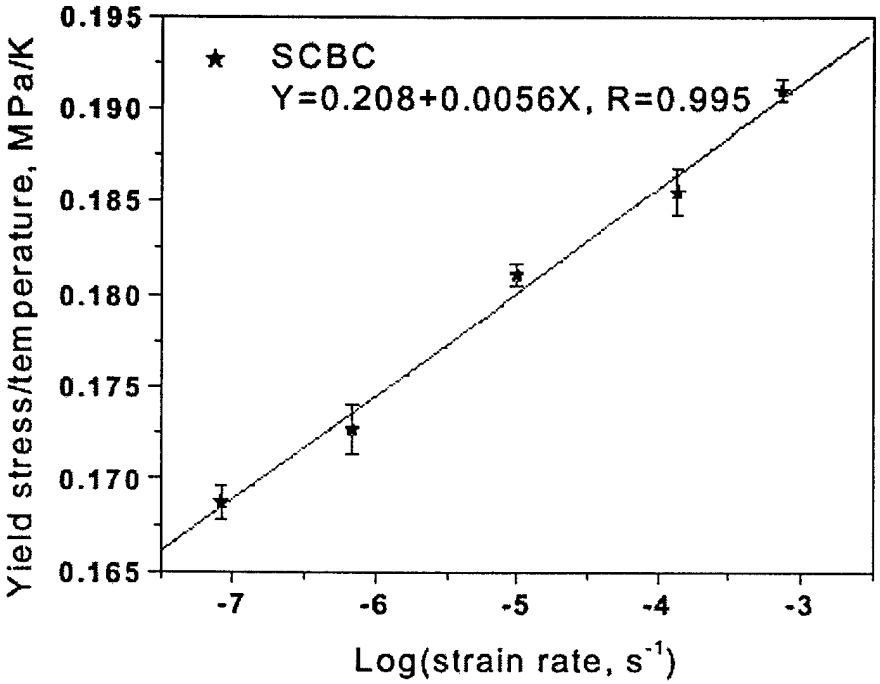


Figure 46: Yield stress versus log strain rate plot at 24°C for SCBC.

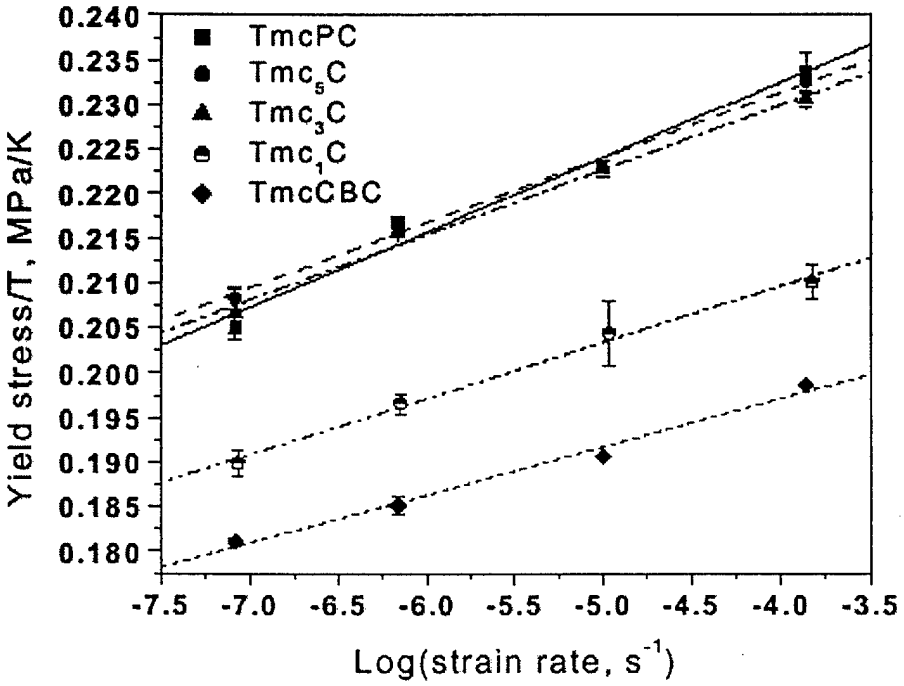


Figure 47: Yield stress versus log strain rate plot at 24°C for Tmc polymers.

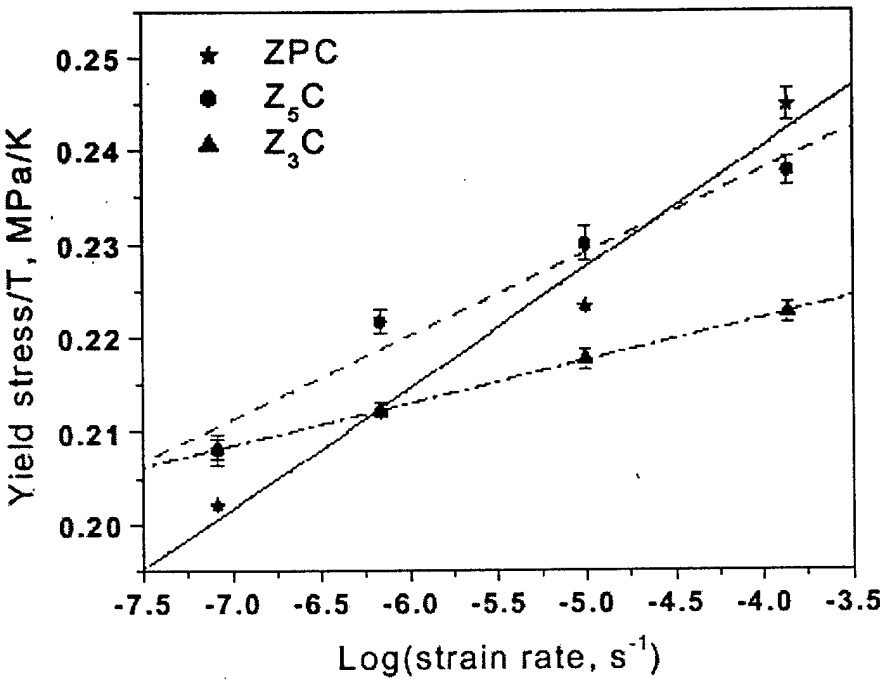


Figure 48: Yield stress versus log strain rate plot at 24°C for BPAZ polymers.

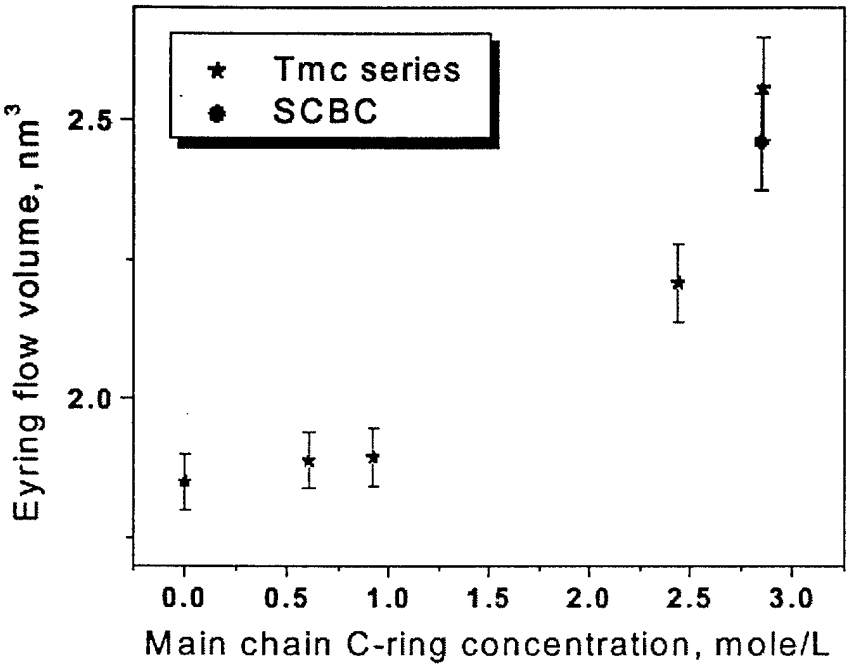


Figure 49: Eyring flow volume for Tmc polymers and SCBC at 24°C.

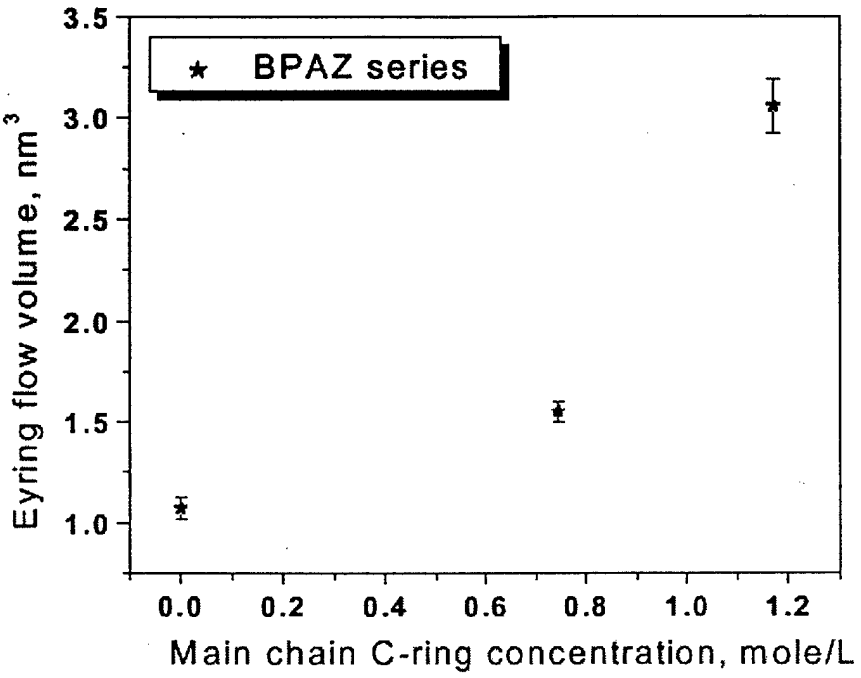


Figure 50: Eyring flow volume for BPAZ polymers 24°C.

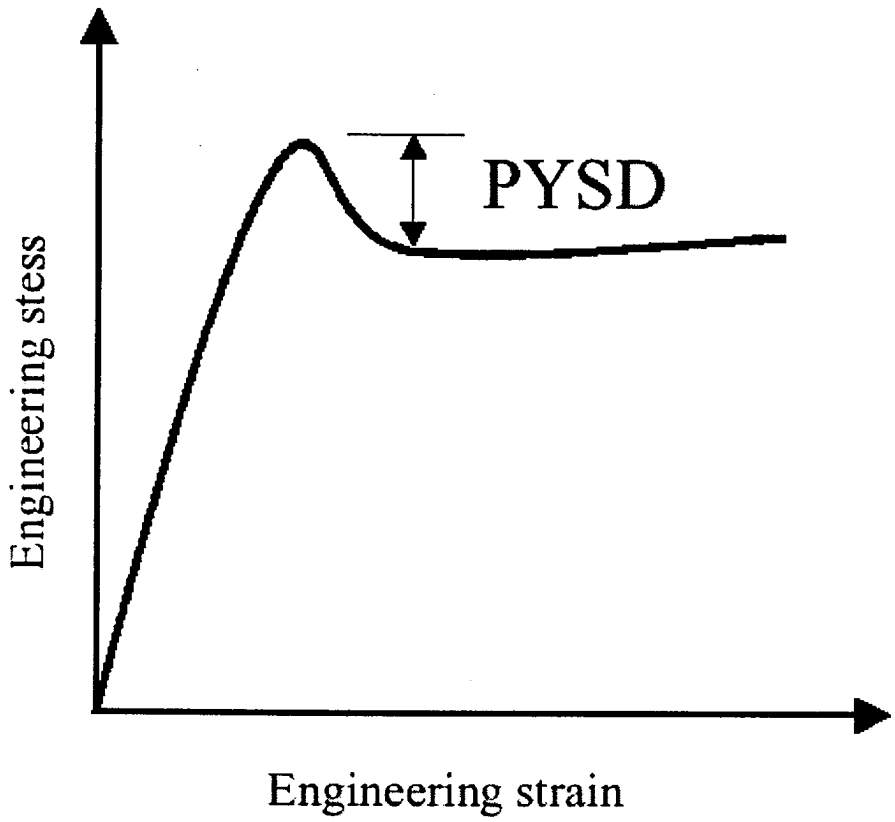


Figure 51: Representation of stress-strain curve showing post-yield stress drop (PYSD).

| No | Polymer | Monomer unit | Tg, °C | $a_o$, $10^{-10}$m | $\bar{l}$, $10^{-10}$m | $\bar{l}/a_o$ |
|---|---|---|---|---|---|---|
| 1 | Kapton(PM) |  | >350(*) | 2.82 | 18.0(**) | 6.4 |
| 2 | DFO |  | 270 | 2.94 | 11.5(**) | 3.9 |
| 3 | H-H |  | 230 | — | 8.6 | ~3.0 |
| 4 | R-R |  | 200 | — | 8.1 | ~2.8 |
| 5 | PPO |  | 170 | 3.36 | 5.6(**) | 1.7 |
| 6 | PC |  | 150 | 3.09 | 2.8 | 0.9 |
| 7 | PET |  | 65 | 2.84 | 2.15 | 0.8 |
| 8 | PS |  | 100 | 4.63 | 1.55(**) | 0.35 |
| 9 | PMMA |  | 110 | 2.85 | 1.55(**) | 0.55 |
| | | | | | | |
| | | * No true glass transition | | | | |
| | | ** Exactly equal to the length of stiff units on the chain | | | | |

Figure 52: Chemical structures and physical properties of glassy polyimides and some previously investigated glassy polymers.[57]

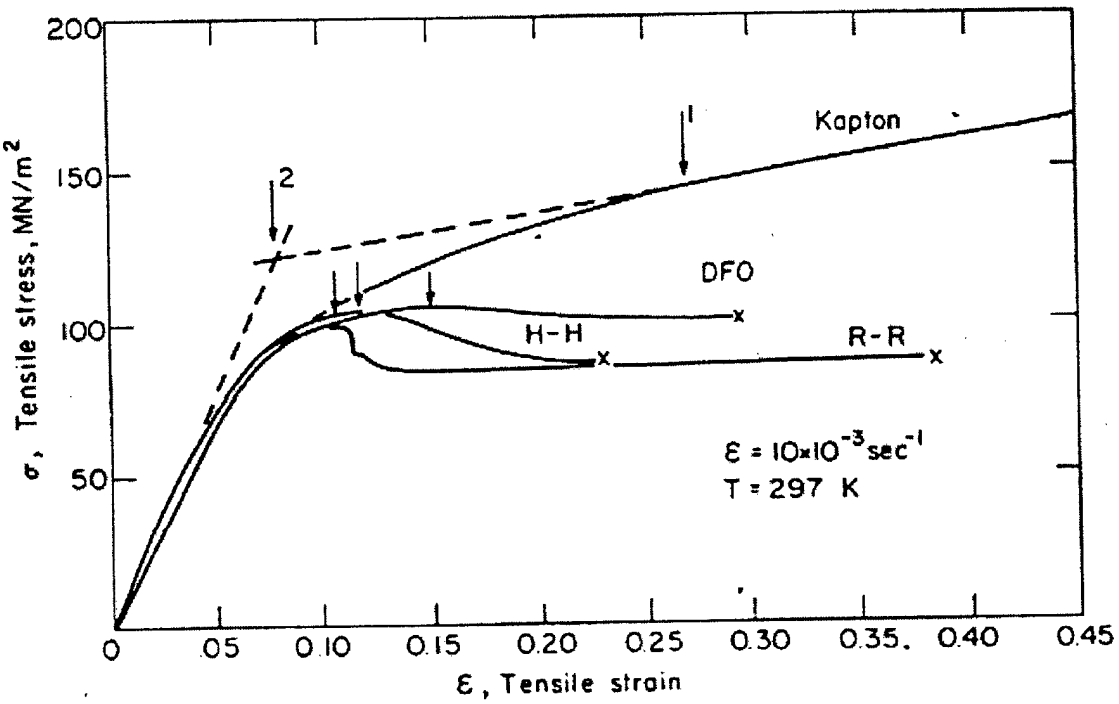


Figure 53: Engineering stress-strain curves in tension for the four polyimide films tested. Arrows shoe positions where yield stresses were evaluated. Crosses show strains where fracture has occured.[57]

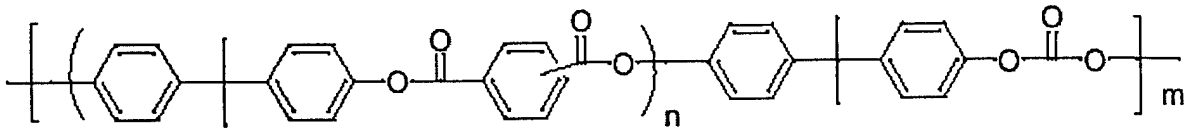

Figure 54: The structures of polyestercarbonates studied by Haward et al..[58]

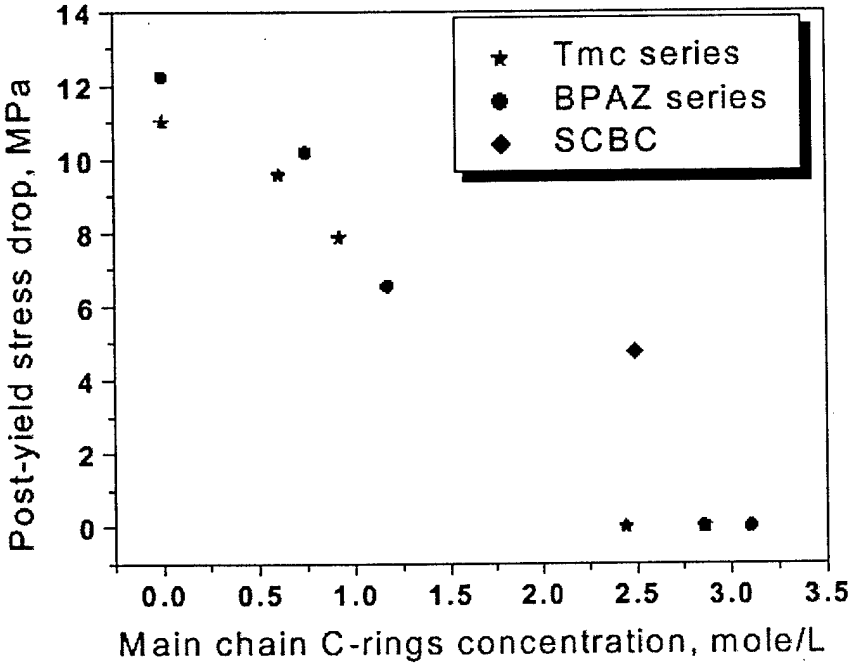


Figure 55: Post-yield stress drop versus main chain C-ring concentration.

Table 1: Molecular weight and glass transition temperature of the polymers.

| Polymer | $M_n$ | $M_w$ | $T_g$/°C |
|---|---|---|---|
| SC | 51k | 778k | 275 |
| SCBC | 39k | 77k | 246 |
| SB | 126k | 262k | 198 |
| TmcPC | 106k | 204k | 240 |
| $Tmc_5C$ | 80k | 137k | 245 |
| $Tmc_3C$ | 75k | 119 k | 252 |
| $Tmc_1C$ | 40k | 84k | 283 |
| TmcCBC | 66k | 131k | 257 |
| ZPC | 32k | 79k | 182 |
| $Z_5C$ | 92k | 164k | 190 |
| $Z_3C$ | 63k | 109 k | 195 |
| $Z_1C$ | 52k | 111k | 228 |
| ZCBC | 87k | 171k | 220 |

Table 2: Molecular weight and glass transition temperature of polymers based on SBI with pure trans C-rings and C-rings with cis:trans=72:28, m stands for mixture of C-rings.

| Polymer | $M_n$ | $M_w$ | $T_g$/°C |
|---|---|---|---|
| SC | 51k | 778k | 275 |
| SC-m | 35k | 49k | 227 |
| SCBC | 39k | 77k | 246 |
| SCBC-m | 31k | 76k | 198 |
| $SC(BC)_2$ | 32k | 63k | 224 |
| $SC(BC)_2$-m | 33k | 83k | 186 |